Ca' Foscari
University
of Venice

Master's degree programme in

Environmental Sciences

Second Cycle (D.M. 270/2004)

Final Thesis

Temporal and spatial dynamics of the nutricline along a repeated transect in the Western Mediterranean Sea

Advisor

Ch. Prof. Bruno Pavoni

Co tutor

Dr. Katrin Schroeder

Graduand

Luisa Fernanda Gordillo Lazarte

Matricul Number 865281

Academic Year

2017 - 2018

Table of contentes

Figures

Tables

Glossary

In alphabetical Order

AB	Algerian Basin
AC	Algerian Current
AEs	Algerian Eddies
AG	Algerian gyre
APB	Algero Provencal Basin
AW	Atlantic Water
DCM	Deep Chlorophyll Maximum
EMED	Eastern Mediterranean Sea
LIW	Levantine Intermediate Water
MLD	Mixed Layer Depth
MS	Mediterranean Sea
MW	Mediterranean Water
ND	Nutricline depth
NSV	Near Sardinian Vein
PB	Provencal Basin
WIW	Winter Intermediate Water
WMED	Western Mediterranean Sea
WMDW	Western Mediterranean Deep Water
WMT	Western Mediterranean Transition

Acknowledgements

First and foremost, I would like to thank my Mother Lucila Silvia Elena Lazarte Rojas for giving me her complete support to achieve this degree. I will not have enough time in my life to thank her for this amazing gesture of love. Secondly, I would like to thank Federico Scavazza for being by my side on this period and for keeping me sane and for all the care and support throughout.

I would like to offer my most sincere appreciation to Katrin Schroeder and Bruno Pavoni for their support during my thesis trials. There is a small and exclusive list of academic superheroes I would like to thank. First a special thanks to Carolina De Los Rios and Eleonora Cusinato for helping me get started and finish, also for all your loving support. I would also like to thank Antonio Petrizzo for all of your MATLAB help. There were several rewrites of code along the way that I would not have been able to overcome without your expertise. It was an honor and a privilege to be able to work alongside.

My Peruvian, international friends, specially Roxana Urquizo and Luisa Blasi and Rita Burchiellaro Scavazza, also deserve a thank you for all the encouragement and for trying to understand what I have been wrapping my head around for the past years.

1. Introduction

1.1. Background and state of the art

Over the last decades, the scientific community is increasing its interest about climate change effects on the ocean features and its consequences on the ocean's trophic levels. For example, it is demonstrated that phytoplankton and zooplankton populations have been altered, and that oceanic carbon capture capacity has been affected by climate change over the last years. Hence, the determination of vertical nutrient fluxes and physical and biological features are of fundamental interest in marine productivity studies (Klein et al., 1984) and a deeper knowledge of nutrient dynamics can be considered as a keystone to understand the negative effects of climate change, which in the future are expected to increase their impacts over a wide range of trophic levels.

Many scientists have been using the Mediterranean Sea (MS) as a laboratory for climate change effects analysis to understand better the ocean's features, as the MS behaves as an ocean in miniature, where the ocean water motions occurs on smaller temporal and spatial scales than those observed in the global ocean (Schroeder et al., 2016). Its study gives an advantageous opportunity to make inferences on global ocean dynamics and processes. More specifically, a deeper knowledge of the nutricline depth (ND) variability in the MS offers a better understanding of nutrient supply for the biological activity in ocean water masses. The ND can be defined using different dissolved inorganic nutrients and it represents the depth at which the vertical gradient of nutrient concentrations is maximum, going from the depleted surface layers (where nutrients are rapidly consumed by primary producers), down to the nutrient-enriched intermediate and deep layers (where nutrients are released during the process of organic matter decomposition). When phosphate concentrations are used, it is called phosphacline, while when nitrate concentrations are used, it is called nictracline.

The MS is well known as an oligotrophic basin by its characteristic low nutrient concentration at the surface. It is composed by three water masses layers, the relatively fresh Atlantic Water (AW) from 0 to about 200 m depth, the salty Levantine Intermediate Water (LIW) from about 200 to about 600 m depth and the Mediterranean Deep Waters (MDW) that can be found below the LIW down to the bottom (Powley et al., 2018). These water masses present different nutrients concentrations, which are typically low at the surface, even though in some specific regions moderate levels of nutrients at shallow depths can be found, due to a number of factors, like spring blooms or upwelling areas (Estrada, 1996).

Numerous researchers looked at different ways to determine the ND, like in 1999 Klein analyzed the nutrient levels in the near-surface waters due to the upwelling of mid-depth waters, which are able to induce enhanced biological activity in the Eastern Mediterranean Sea (EMED), providing nutrients to the euphotic zone. The author defined the ND as the region within the strongest concentration gradient between the nutrient-deprived surface waters and nutrient enriched deeper waters below, where nitrate concentrations reach a fixed threshold of 3 µmol/kg (the value varies depending on the region). During summers seasons in 1992 and 1999, coastal samples were analyzed by Laanemets et al. (2004), in their research work developed in Finland (Western Gulf), over a region with physical processes clearly affected by wind forces, concluded that the seasonal variability of ND was due to seasonal dynamics of phytoplankton biomass and species composition together with nutrient conditions (interannual changes in external and internal loads), in which mesoscale physical processes induce reversible movements of the ND. A wind-induced turbulent mixing and coastal upwelling transport

nutrients with a very low nitrate to phosphate ratios into the upper layer were also noticed, as a consequence of the vertical separation of the phosphacline and the nitracline. A different point of view was proposed by Cermeno et al. (2008), who examined microscopic plankton species of four meridional regions in the Atlantic Ocean, showing that the biological activity displacement is linked with the ND. The ND is used as an indicator of nutrient availability at upper mixed layers if the water column and of the phytoplankton community composition. In relation of the nutricline, they found that in upwelling oceanic areas and temperate regions with higher latitudes, the major amount of nutrients is brought by wind-driven vertical mixing and are carried along isopycnal layers, from deep water layers. Biological activity at lower latitudes (stratified subtropical gyres), can be recognized as highly dependent on the resident recycling and diapycnal nutrient flows, for a moderate growth of biological population. Some of the organic matter produced by the biological activity, manages to sink acting as a biological pump, entering into the deep layer where it will be remineralized and transformed again in carbon dioxide, which eventually returns to the atmosphere, by bacteria activity (Cermeno et al., 2008; Liu et al., 2008). Hence, the availability of nutrients for biological activity is considered a critical factor in the regulation of the global carbon cycle.

Despite several studies about the MS biogeochemical oceanography carried out over the last decades (e.g. Bethoux, 1998; Kress & Herut, 2001; Ribera d'Alcalà, 2003; Marty & Chiavérini, 2010; Olita et al., 2013; Pasqueron de Fommervault et al., 2015; García-Martínez et al., 2018; Powley, et al., 2018), information related to biological processes, seasonal and inter-annual dynamics of nutrient concentrations and ND displacement on the water column remain poorly known in some areas of the MS.

In the present thesis, the main focus will be the spatial and temporal variability of the ND, analyzed along a repeated transect between Minorca and Sardinia, which has been carried out with Italian Research Vessels between 2005 and 2015. Moreover, the interaction of the Mixed Layer Depth (MLD) with nutrients availability and biological activity, which can be strong in many regions of the ocean, will be analyzed, since the MLD can be used as an important proxy for ND and phytoplankton activity studies. Finally, also the interaction between ND and the depth of the Deep Chlorophyll Maximum (DCM) will be investigated in order to determine the interlink of phytoplankton vertical dynamics and nutrient concentrations in different years and in different seasons.

1.2. Study Area

The western Mediterranean (WMED) is well recognized in the scientific community by its reduced dimensions in comparison to the ocean and its contribution to the global heat and freshwater balance (Vargas-Yáñez et al., 2010). This basin presents considerable heterogeneity, due to several hydrographic features its potential phytoplankton fertility can be observed at high levels (Estrada, 1996), as an example, winds from the north and the northwest strongly modify temperatures and salinities of the Gulf of Lion (Champalbert, 1996). The latter facts are just some of the numerous facts that make the WMED an advantageous region for climate change recognition studies and monitoring programs. The WMED has a well-known oligotrophic character, by the exchange of water with the Atlantic Ocean through the Gibraltar Strait (exports nutrient-rich waters / imports depleted nutrient surface water) (Volpe et al., 2012). The WMED comprises the Alboran Sea, the Algerian Basin, the Provencal Basin, the Balearic Sea and the Tyrrhenian Sea (Lort, 1977).

The samples were taken during repeated cruises along a zonal transect (Table 1) between Minorca and Sardinia in the Algero-Provencal Basin (APB, Figure 1). The samples were collected from 2005 to 2015 during seven cruises, covering the entire water column, from top to about 2500 m depth, near the seafloor.

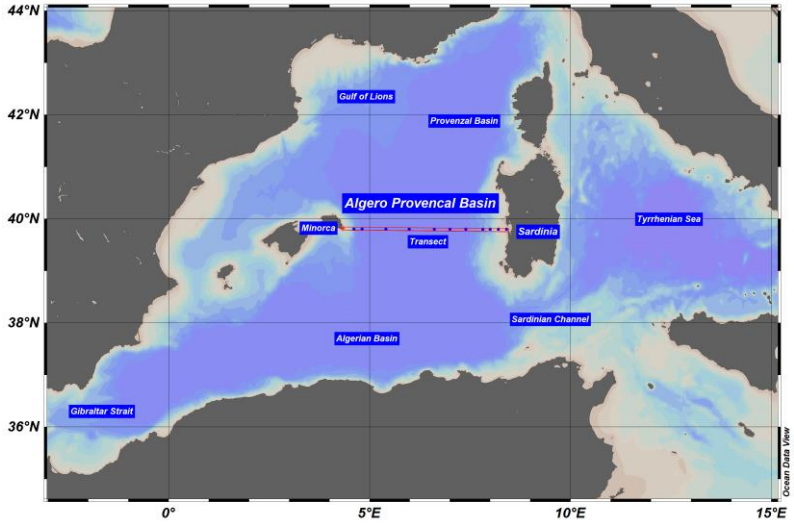

Figure 1. Map of the WMED and location of the stations between Sardinia and Minorca.

Table 1. Minorca –Sardinia transect geographical limits.

Zone	Latitude	
	Ending	Beginning
North	39.804	39.803
West	4.405	7.998

1.3. Relevant levels in the Sea

In this section we will define and describe the three layers or levels which dynamics is the subject of this thesis. These are the Mixed Layer, the Deep Chlorophyll Maximum and the Nutriclines.

1.3.1. Mixed Layer

The Mixed Layer (ML) is a turbulent homogenized oceanic layer generated by active air-sea exchanges, situated in the shallower region of the ocean. These air-sea exchanges enhance the surface turbulence (water mixing) and leave salinity, potential density and temperature homogeneously mixed. Thus, the ML is expected to be a quasi- homogeneous region in the upper ocean, which can experience small variations of temperature, potential density or salinity with depth (Kara et al., 2000; Sprintall & Cronin, 2009). A minimum vertical property gradient can still take place in the interior of the ML in response to, for example, adiabatic heating or thermocline erosion. A further important fact on the ML depth (or MLD) analysis is that over the first 10 meters diurnal signal can lead to an error in the MLD identification (Fine et al., 2015).

The main source of the oceanic motions is the heat, mass and momentum exchange between the air and the sea (Figure 2). Whereas the vertical mixing region is due to wind, surface cooling, wave energy, current shear and other physical phenomena interactions, the depth of this homogeneous and neutrally buoyant layer can be highly variable, because it represents a balance between stabilizing forces (e.g. by heating in summer) and destabilizing forces (e.g., by

cooling in winter, Cronin & Sprintall, 2009). Consequently, the MLD can be affected by particular events and its regular seasonal variability can be modified.

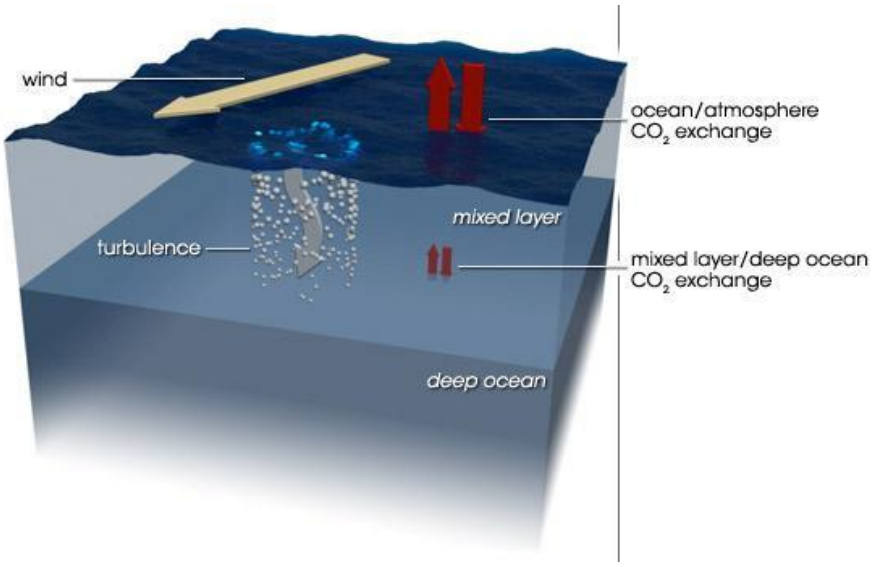

Figure 2. Normal Ocean Stratification (from *https://earthobservatory.nasa.gov/features/OceanCarbon*).

The general key processes capable to generate fluctuations in the MLD are heating, cooling, mixing and lateral advection. Its predominant temporal scales of variability are seasonal, monthly, diurnal and semidiurnal, tidal, short periods and random variations trough mixing (Huthnance et al., 2001). Approximately from December to April the vertically mixed season takes place (absence of the seasonal thermocline) where the MLD reaches its maximum depth (colder and denser surface layer). In specific locations, like in the Gulf of Lion in the northern WMED this process can reach extreme depths, bringing the MLD down to > 2000 m during the process of deep-water formation. The stratified season takes place approximately from May to November (formation of a strong and shallow seasonal thermocline), where the MLD reaches its minimum depth (less dense and warmer surface waters). In accordance with Houpert et al., (2015) in the MS the MLD shows higher depth values from January to March, attributable the deepest displacement of the mixed layer, while re-stratification of the water column starts in April in which the MLD stays at moderate depth levels (than 30–40 m). From late autumn to early winter (September – December) MLD standard deviations values generally stays under 30 m for almost all the basin, the standard deviation exhibits highest values during winter and April (whole basin). An important feature of the MLD has been reported by Houpert et al. (2015) who show that the deepening of the ML did not start exactly at the same time and the time lag between different years, time lags can by around the 1.5 months. Gyres (cyclonic/anticyclonic) also affect the MLD, with anticyclonic gyres tending to push down the thermocline, and cyclonic gyres tending to push it upwards. Since the MLD is defined on the base of temperatures gradients, the gyres affecting the thermocline depth also affect the MLD.

1.3.2. Deep Chlorophyll Maximum

The Deep Chlorophyll Maximum (DCM) is defined as the subsurface depth range over which the chlorophyll peak occurs (Beckmann & Hense, 2007; Hanson et al., 2007; Jobin & Beisner, 2014; Platt et al. 1988). The DCM has been recognized as an important ecological hot spot of primary production and nutrient cycling, and its location can determine vertical habitat gradients for the primary production. Likewise, the DCM is frequently associated with thermocline and low light areas, with 1–3% of the incident surface photosynthetically active radiation (PAR).

The DCM distribution is affected by the WMED dynamic behavior and nutrients availability supplied from the layers where the nutriclines are located. Its hydrodynamic processes may strongly influence the phytoplanktonic distribution and concentration (Morán et al., 2001). It is likely that this parameter may interact with other parameters of the WMED, like the ND (nitracline and phosphacline) or the MLD (vertical mixing can supply nutrients to the upper layers).

The main mechanisms of the DCM formation and maintenance include the enhanced growth with light and nutrient availability, fitting modifications of organic processes in the chlorophyll-rich layer, moving to lower depth levels and accumulation at intermediate oceanic layers behavioral accumulation of mobile planktonic species, internal currents, selective feeding consumption, turbulent mixing, and horizontal intrusional intermediate oceanic layers (Cullen, 1982). In very simple terms the subsurface depth where the chlorophyll concentrations peak is the result of a tradeoff between high light levels at the surface (but low nutrient levels) and high nutrient levels going deeper (but low light levels). The DCM is then located where both light and nutrient availability are high enough to support growth of primary producers.

The seasonal oceanic geophysics system oscillates from mixing season (January–February) to robust stratification season (summer to autumn). During summer are exhibit strong oligotrophic conditions (nutrients depleted /surface layer), while in winter occurs the re-injection of nutrients at surface layer (Marty et al., 2002). The depth of the DCM increases from spring to summer (Estrada, 1996), reaching its maximal depth at summer driven by sunlight. During winter the DCM reaches its shallowest depths, due to a photoacclimation to the reduced irradiance (Mignot et al., 2014), and because of vertical mixing enabling enhance nutrient supply to the surface layer.

In the northern WMED some regions with particular strong spring blooms can be recognized, as the Gulf of Lion. D'Ortenzio & D'Alcalà, (2009) report that the duration of the bloom in this region take place in a four-phase pattern: an early rise in winter (November–December), continuing with a mild reduction during winter (first months of the year), followed by the progress of an annual peak in early spring, finally decline from late spring to early summer. This four-phase pattern is normally detected along the ten years of their investigation, where the interannual variability plays a significant part in changing the extent of the four phases.

1.3.3. Nutricline

The nutricline is located where the vertical rate of change of a nutrient concentration is maximum, that represents the boundary between the region of the water column where the nutrients are depleted (surface layer) and the deeper region of the water column where nutrients are present in high concentrations. Depending on which nutrient is used to determine it, we can speak about the nitracline (using nitrate concentration vertical gradients) and the phosphacline (using phosphate concentration vertical gradients). According to Cermeno et al. (2008) the ND can be used as an optimal indicator of nutrient availability at the upper ML of the ocean water column. For this reason, phytoplankton primary production is inversely related with the depth of the nutricline, a negative relationship that denotes a strong connection with the nutricline position in the ocean layers, the amount of nutrient concentration into the euphotic zone and biological activity efficiency. Studying the nutricline dynamics or projecting them into the future might give important hints on how the ocean carbon cycle is or will be affected by climate change.

Laanemets et al. (2004) highlighted the seasonal feature of the nutricline, which depth, separation (between nitra- and phosphacline) and gradient are probably determined by seasonal dynamics of phytoplankton biomass and species composition with changing nutrient conditions (interannual changes in external and internal loads). Furthermore, mesoscale physical processes might induce displacements and intrusive layering of nutriclines. The separation of the phosphacline and nitracline essentially influence the vertical displacement of nutrients (NO_3 and PO_4) by upwelling and strong mixing, because where the two layers are not coupled an anomalous N:P ratio is found.

According to Cermeno et al. (2008) the stratification level in the water column and the extent of air-sea momentum (by wind stress), strongly affect the nutricline position in the water column. Moreover, when winter mixing became stronger, the upper mixed layer enters in the nutricline layer, thereby transporting the nutrients from the ND to the photic layer, with nutrient levels becoming elevated throughout the upper water column. Conversely, when thermal stratification increases (from late spring to early autumn), the ocean shallow region is nutrient depleted, which generates deeper displacement of the nutricline that can be recognized parallel to the deepening of the DCM.

1.4. Objectives and thesis outline

In the present work, physical and biogeochemical measurements carried out during seven cruises conducted along a transect between Minorca and Sardinia, in the central area of the Algero-Provençal Basin (APB), by the Marine Science Institute of the Italian National Research Council (CNR-ISMAR) are used to perform the analyses of the distribution of physical (potential temperature, salinity and potential density) and biogeochemical (fluorescence, nitrate and phosphate) parameters.

The main goals of this study are:

(a) To quantify temporal (seasonal and interannual) and spatial variability of the ND.
(b) To identify controlling factors on the ND and, consequently, on the primary production: i.e. eddies, wind-surface current interaction, seasonal variations of the physical (salinity, density, temperature, MLD) and biological (DCM) factors.

The thesis is arranged as follows: the first chapter includes the introduction, background and state of art, study area and the description of the ocean layers that are relevant for this study (ML, DCM, nutriclines). The second chapter is a description of the WMED, its circulation and water masses as well as its biogeochemistry. The third chapter describes the data, methodology and tools used for the analysis of the ND, the DCM and the MLD. The fourth and fifth chapters describe the results and discussion, while conclusions are given in the last chapter.

Appendixes are reported to have an overview about the MATLAB codes used to perform all the analyses of this research. They are arranged as follows: Appendix 1 provides the routine for estimating the ND based on the nitracline and phosphacline in MATLAB; Appendix 2 describes how to plot the DCM, MLD and NC for each cruise in MATLAB; Appendix 3 illustrates the MATLAB script used to read interpolated data exported from Ocean Data View (ODV), while Appendix 4 contains the MLD computational method.

2. The Western Mediterranean

The MS is a mid-latitude semi-enclosed sea (Figure 3) where several essential processes for the global ocean circulation happen equally or in a very similar degree (Robinson et al., 2001). The MS represents 0.8% of the global ocean surface (Catalá et al., 2018). It is connected with the world's oceans through the narrow Strait of Gibraltar (Lascaratos et al., 1999), a sill with a depth of 284 m (Bryden et al., 1994). On the eastern side, it is connected to the Black Sea by the Dardanelles and Marmara Sea Straits systems. Its surface is approximately 2.51 million km^2 with a width of about 6000 km and it is bordered by Europe to the North, Asia to the East and Africa to the South.

The MS circulation has been studied for more than five decades and is thought to be driven by the convection phenomena, connecting intermediate and deep layers to the surface at a few specific sites where dense water formation occurs (Waldman et al., 2018). Béthoux et al. (1979) highlighted the particularly negative water balance of the MS (precipitation < evaporation), while Lascaratos et al. (1999), emphasized the hydrological characteristics of the basin given by the inflowing Atlantic low salinity water and the heat budgets. The anti-estuarine circulation is given by AW flowing eastwards at the surface, entering through the Gibraltar Strait to the MS. Along its path to the East, losing progressively its characteristics through mixing and evaporation (Lascaratos et al., 1999), it is transformed into saltier Mediterranean Water (MW) (García-Martínez et al., 2018) which exits into the Atlantic Ocean via the lower layer within the Strait of Gibraltar.

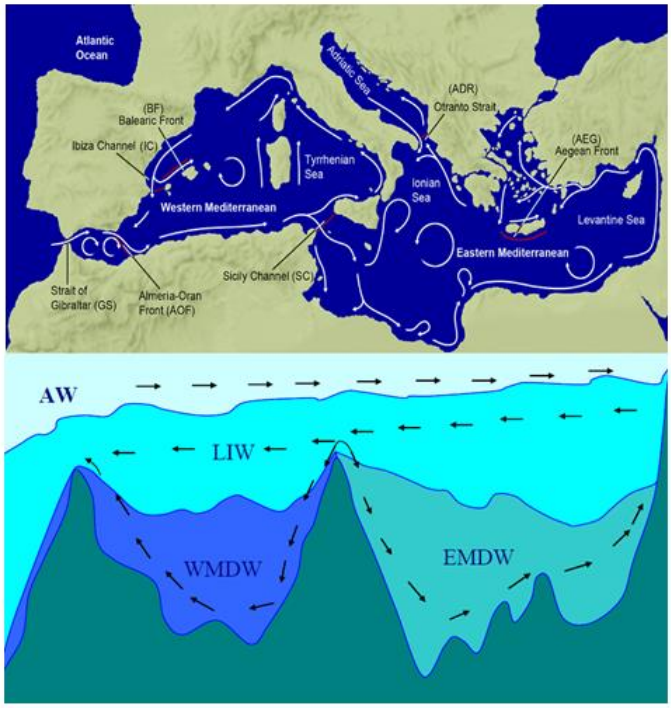

Figure 3. The Mediterranean Sea, its sub-basin (top of the figure; Pascual et al., 2017) and main currents and its vertical layers (bottom of the figure).

The Sicily Channel divides the MS in two basins, the Western Mediterranean Sea and Eastern Mediterranean Sea (WMED and EMED). The WMED presents small differences in the distribution of temperature, salinity and dissolved oxygen within its sub-basin. It is composed by the Algerian Basin (AB), the Provencal Basin (PB), the Alboran Sea, the Catalan Sea, the Tyrrhenian Sea and the Ligurian Sea. The transect used for this study is located in the APB

(between the Provencal and the Algerian Basin). The APB represents one of the most dynamic areas of the entire MS and, for this reason, its hydrodynamics have been intensively investigated (e.g., Olita et al.,2011). During the last decade, a considerable amount of scientific research has been developed in regard of the WMED circulation and results obtained confirm the Millot's (1987) diagram (Figure 3).

2.1. Circulation, water masses and eddy dynamics in the WMED

Since the mid '80s, the WMED has been experiencing an increase of salinity and temperature levels. Schroeder et al. (2016) present an analysis of the evident increasing level since 2005. Schroeder et al. (2008), distinguished anomalously severe winters (2004-2005 and 2005-2006) that lead to major deep-water formation, in which high-salinity, high-temperature and high-density deep waters were formed, setting the beginning of the Western Mediterranean Transition (WMT). The MS experience a substantial salinification process since the 1950s, in accordance with the water cycle (global ocean) increase size and the salinity average pattern, (Bethoux et al., 1999; Rohling & Bryden, 1992; Schroeder et al., 2016; Skliris et al., 2018; Vargas-Yáñez et al., 2010).

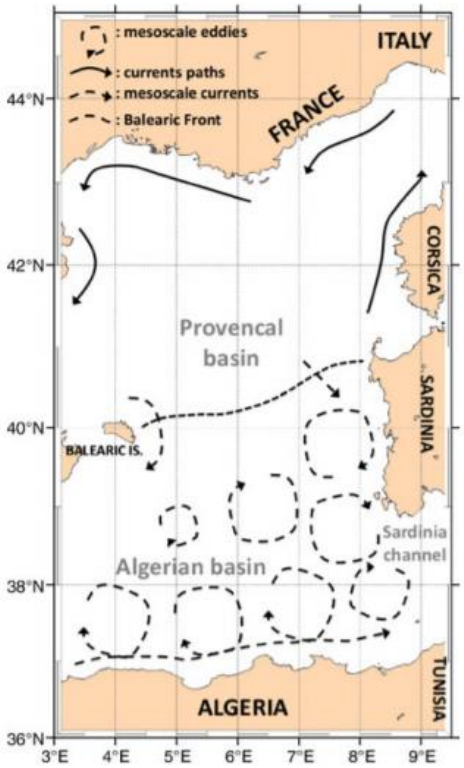

Figure 4. APB and the main dynamical features and geographical regions s; Current paths (->), Mesoscale currents (-->) (Olita et al., 2011).

Intense mesoscale and sub-mesoscale variability interact across sub-basin and basin scales (Gómez-Navarro et al., 2018), and they have an intense effect on physical and biogeochemical parameters of the water masses. Millot (1999) reports definitive results about the mesoscale phenomena in the APB (Figure 4), which induces a dramatic variability of the circulation of the water masses near the Balearic Islands and through the Sardinia Channel. The area is known for its intensive mesoscale activity giving rise to a variety of eddies up to 200 km in diameter (Millot, 1987; Karimova, 2018; Levy et al., 1998; Olita et al., 2011).

The APB is a region of the WMED mainly composed by three sub-regions, the AB (south), the PB (north) and the buffer (center) region between the two basins. In the AB, at the surface, the AW inflowing from the Gibraltar Strait is found. Along the Algerian coast the AW flows eastwards by the Algerian Current (AC), in which anti-cyclonic Algerian eddies (AEs) are generated by baroclinic instabilities of the AC (Obaton et al., 2000). Also, the northern region (PB), present a high dynamic region with strong mesoscale activity. In the buffer region between the AB and the PB, the Northern Balearic Front (NBF) has been recognized to be a semi-permanent feature (Lopez Garcia et al. 1994; Millot, 1999; Olita et al., 2011; Pessini et al., 2018; Pinot et al., 1995). The NBF has its origins close to the Balearic Islands, due to the inflowing waters of recent AW through the Balearic sills, which has been partially deflected by anticyclonic eddies from the AC. The signature of the NBF is a vigorous salinity jump of about 0.6 (37.4 to the South and 38.0 to the North) down to 150 m depth. This distinctiveness salinity identifies the front as the main transition zone between two water masses, which in winter is detectable with satellite images with a weak detectable temperature gradient (0.5-1 K/5 km) (Mancho et al., 2008).

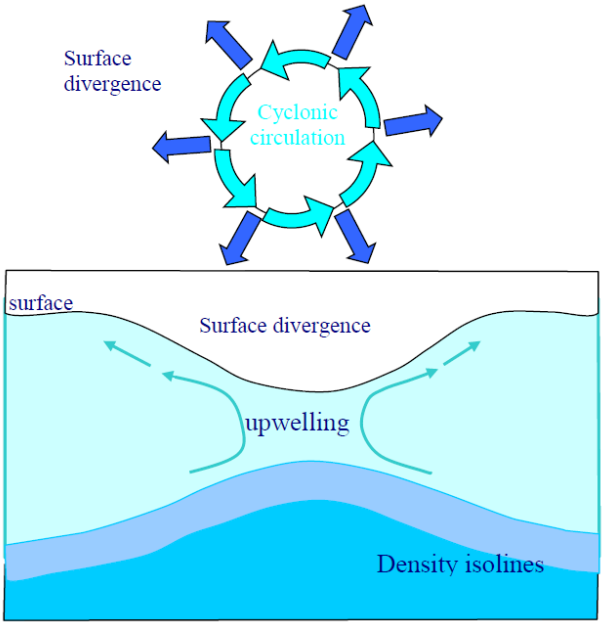

Figure 5. Cyclonic circulation effects on upwelling and density isolines (in the top panel the distribution of currents is shown from above, in the bottom panel their effect on a vertical section).

Generally, in the Northern Hemisphere, a current moving counterclockwise (cyclonically) generates a divergent gyre, which means that surface waters tend to move from the center of the vortex towards the outside of the vortex. This induces a lowering of the sea surface at the vortex center. This “lack of water” has to be compensated, in force of the continuity equation of water, by water coming from the deeper layers: this behavior is called “upwelling”. The opposite phenomenon (occurring when the vortex is anticyclonic) is called “downwelling”, which occurs in convergence areas. The upwelling of deeper waters produces an upward lifting of the thermocline, that is a doming of the isolines of temperature, salinity and density, to compensate the horizontal pressure gradient (see Figure 5). A large-scale oceanic divergence region can be seen from satellite images, with the upwelled waters being generally richer in chlorophyll (because they are nutrient-enriched). Cyclonic eddies normally stimulate biomass growth due to remarkable upwelling of nutrient-rich water in their cores (e.g. McGillicuddy et al., 1998). While anticyclonic may enhance bio-productivity, by strong upward velocities on their edges, shallow water mesoscale vortices on a coastal slope generate a complex pattern of strong

vertical velocities, linking nutrient-rich deep waters and the nutrient-depleted upper layer (Karimova, 2018).

Typically, the AEs lifetime can be from a few months (Millot, 1987) to 3 years (Puillat et al., 2002) and they move around the AB in a 1-year average time (like a 1-year loop). The AEs are originated due to the baroclinic instability (Obaton et al., 2000) of the AC (Figure 6), providing appropriate conditions for the origin of large anticyclonic AEs nearby 1–2° E, as noticed by Testor & Gascard (2005), which can extend from the surface down to about 350 m depth (maximum depth reached by AW in this area). However, they can develop over deeper depths during particular episodes. Near 8° E, cyclonic AEs with a mean speed of few cm s^{-1} were detected, detaching from the Algerian slope, frequently before arriving at the Sicily Channel. Only anticyclonic structures seem to grow and become large and energetic (Testor & Gascard, 2005). Additionally, the distinctive AB local topography, analyzed by Rio et al., (2014), seems to enhance the formation of the AEs (both cyclonic and anticyclonic).

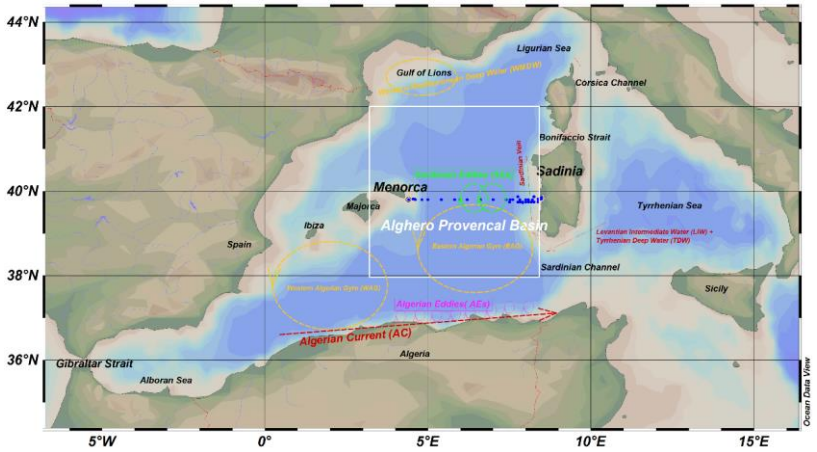

Figure 6. Right dotted orange circle delineates the shape of Eastern Algerian Gyre found by Testor & Gascard (2005), occupying a large part of the AB between the Balearic Islands, Sardinia, and North Africa.

Testor & Gascard (2005) analyzed the inflowing water masses from the Tyrrhenian Sea to the APB along the northern side of the Sardinia Channel, where a main core of LIW has been perceived, with a center near 350 m depth (temperature and salinity maxima), which flows westwards and then turns northward. Also, Tyrrhenian Deep Waters (TDW) has been detected outflowing from the Tyrrhenian Sea to the Algerian Sea along the Sardinian coast (Send et al., 1999). TDW is formed within the Tyrrhenian, where LIW mixes with the WMDW.

According to Testor & Gascard (2005) in the APB can be recognized a strong seasonal variability of a winter anticyclonic Sardinian Eddy (SE) vorticity formation, between the Algerian Gyre (AG) and the general boundary circulation entraining LIW along the continental slope of Sardinia (Near Sardinian Vein, NSV). The rotational period of the SE is around 3–4 weeks (radius ~ 30 km), which evolves in the AG periphery. It is composed by LIW (at 600 m depth in the core of the eddy) and the same features of the LIW are present along the slope west of Sardinia. Between the AG and the circulation along the continental slope, south-west of Sardinia where the AG and the NSV merge and then split, the origin of the SE was detected. SE enhances the spreading in the APB of recently mixed LIW and TDW coming from the Tyrrhenian Sea. The NSV (along the Sardinian coast) northwestward flow is probably affected by the SE, spreading the westward inflowing Tyrrhenian waters through the APB. Each year 4 to 5 well developed SEs can be detected, which are responsible of 50 % of the inflowing waters though the Sardinian channel. Frontal eddies (FEs) where described by Fuda et al., (2000): they typically carry Winter

Intermediate Water (WIW) and LIW. The majority of the FEs have a short period of live and travel westward at a few kilometers per day along the NBF (Pessini et al., 2018). These authors report eddies seasonal variability, detecting a winter peak of short lifetime cyclonic and anticyclonic structures, which are usually homogeneous (< 90 days).

2.2. Biogeochemistry of the WMED

The MS is vastly recognized as an oligotrophic basin, with its oligotrophic character increasing eastwards, due to its anti-estuarine circulation (Tanhua et al., 2013). The anti-estuarine circulation is driven by the surface AW inflow with relatively low inorganic P and N concentrations (and with higher molar NO_3:PO_4 ratio than the Redfield ratio 16:1), and the outflow of deeper waters enriched in dissolved inorganic nutrients. Notwithstanding, the WMED have moderate levels of primary production (higher than the EMED), named by Sournia (1973) as the "Mediterranean paradox" (Segura-Noguera et al., 2016). The inconsistency mention before, was elucidated by Estrada (1996) and later by Garcia (2006), which found that the nutrient moderate levels at the surface layer was based on the regenerated production, maintained at moderate levels by the nutrients injection from the atmosphere and land runoff, as well as by the contribution of irregular fertilization at the ocean water column (i.e. frontal zones) and N_2 fixation. However, the source of N and P which makes the difference in primary productivity between the EMED (lower) and the WMED (higher), is the higher marine inputs in the WMED than in the EMED, causing 3 times higher primary production in the WMED (Powley et al., 2018). These authors also report important differences between the two basins with respect to the deep waters, molar NO3:PO4 ratio, being lower in the WMED than in the EMED, which demonstrate that the inputs into the WMED have less reactive N:P ratios, including a rather low N:P ratio of Atlantic surface water entering in the MS.

Nutrient limitations are present both in the WMED (where they are less intense) and in the EMED. This limitation is mainly due to low availability of phosphorus. In the WMED in some particular regions the phytoplankton bloom is quite intense and is typically initiated by mixing of the water column, which brings NO_3-enriched water (with NO_3: PO_4 > 16) into the photic zone (Severin et al., 2014).

3. Data and method

3.1. In situ data along a repeated transect

The on-board operations (CTD casts), on all cruises and at all the hydrological stations, measure pressure, potential temperature, salinity, fluorescence and dissolved oxygen concentration with a CTD rosette system residing of a CTD SBE 911 plus, and a General Oceanic rosette with 24 12-l Niskin Bottles. In *Figure 7*, the displacement of the stations along the sampling transect is shown.

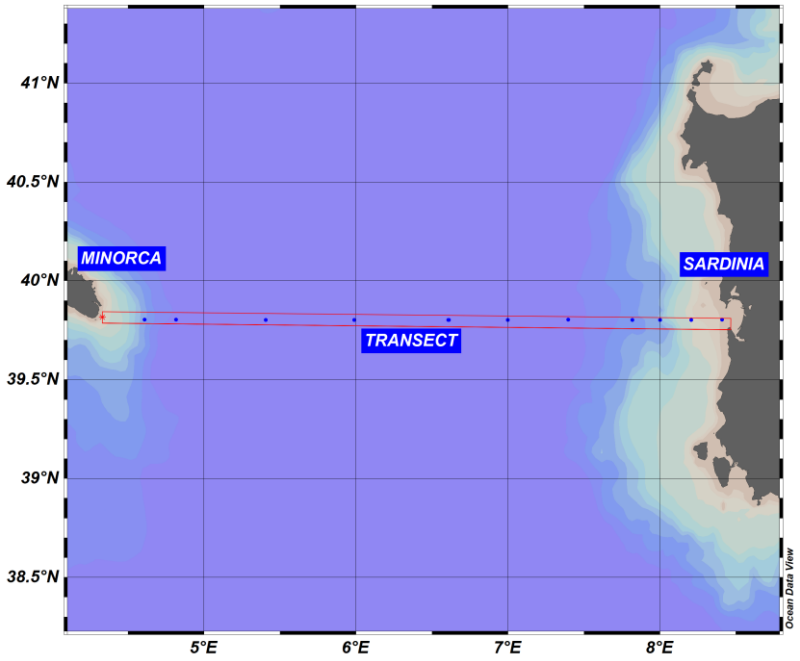

Figure 7. CDT Stations between Sardinia and Minorca.

The biogeochemical datasets used in the present study were acquired from the databases of CNR-ISMAR (Belgacem et al., in preparation), taken on the following cruises: Cruise 1 (spring 2005), Cruise 2 (summer 2006), Cruise 3 (autumn 2007), Cruise 4 (spring 2010), Cruise 5 (autumn 2011), Cruise 6 (winter 2012) and Cruise 7 (summer 2015) on board the Italian vessels RV Urania (2005-2012) and RV Minerva Uno (2015). The nutrient data collected in 2008 and 2013 were too scarce and could not be used for the analysis, while in 2009 no samples were collected. In the following Table 2 the cruise specifications are described.

Table 2. Cruise List. The original names of the cruises are reported as well but for this thesis research purpose these cruises names were modified with IDs from #1 to #7

Cruise name	Expedition dates	Cruise Name
Cruise 1	7 - 9 May 2005	MEDOCC05
Cruise 2	17 - 19 June 2006	Medocc6
Cruise 3	16 - 18 October 2007	MedOcc7
Cruise 4	10 - 12 May 2010	Biofun2010
Cruise 5	16 - 18 November 2011	Bonifacio2011
Cruise 6	17 - 18 January 2012	Ichnusa2012
Cruise 7	10 - 22 August 2015	Oceancertain_15

Sampling groups working together on board, measured different parameters, with different instruments and methods defined in Table 3. The CTD stations have been chosen both on historical basis. CTD, oxygen and fluorescence measurements have been made during CTD casts, providing hydrological information about the area. Samples have been taken in bottles in order to determine dissolved oxygen and salinity (on board) and then nutrients (just sampled and frozen, analyzed in the laboratories onshore). In order to achieve information about the spatial variability of this parameters, a sampling has been applied at standard depths (Table 4). Extra sampling depths have been defined in the water column by analyzing the CTD profile during the acquisition, if needed.

Table 3. Sampling equipment and analysis methods

Instruments	
Small-Volume Sampling	General Oceanic 24-place rosette with 12 L bottles
CTD	SBE 911 plus
Fluorimeter	AQUAtraka MK III
Salinometer	Portasal Guideline
Dissolved oxygen	Winkler titration with Titrino SBE 43
Nutrients	Only samples frozen on board

Table 4. Sea water samples for dissolved inorganic nutrient measurements at standard depths (at 50% of all CTD casts.)

Level	Standard depth (m)
1	0
2	25
3	50
4	75
5	100
6	200
7	300
8	400
9	500
10	750
11	1000
12	1250
13	1500
14	1750
15	2000
16	2250
17	2500
18	2750
19	3000
20	3250
21	3500

Frozen nutrient samples (stored at −20 °C) were brought to the ENEA laboratory (La Spezia, Italy) and the chemical analysis for all dissolved inorganic nutrients were carried out, for the determination of nitrate and orthophosphate concentrations have been used a Brän–Luebbe AutoAnalyzer standard procedures (Grasshoff et al., 1999), with slight modifications. The nutrient data quality is assured through the successful and continuous participation of the ENEA-CRAM laboratory to the European intercalibration programme QUASIMEME (Quality Assurance of Information for Marine Environmental Monitoring in Europe, see Topping, 1997). Analytical errors for the measured parameters are ±0.005 µmol dm^{-3} for phosphates and ±0.01 µmol dm^{-3} for nitrates (Schroeder et al., 2010).

3.2. Determination of the MLD

Based on the method described by Lorbacher et al. (2006), the MLD is computed as the "*shallowest extreme curvature of near surface layer density, salinity or temperature profiles*", as was defined by the author of the method (h_{mix} or MLD). The general method computes the vertical gradient (gT, Equation 1) with respect to a level 5 m deeper (for this research propose the depth was modified in some stations) and the curvature (cT, Equation 2). The depth z(i) is defined as negative, with i being equal to one, as the closest level to the surface. Vertical profiles slope (or gradient) at level i are determined, where the index *i5m* denotes the next deeper level, being almost 5 m greater than the level i, to obtain a more stable estimate gT. The gradient gT(i) is defined as the slope below the level i; gT is positive if T (T can be potential density or salinity or potential temperature) declines with depth.

$$g_T(i) = \frac{T(i) - T(i5m)}{z(i) - z(i5m)} \quad \textit{Equation 1}$$

The curvature ($cT_{(i)}$) is centered and positive if gT above the current level is smaller than gT of the current level (Equation 2).

$$c_T(i) = \frac{g_T(i) - g_T(i-1)}{z(i-1) - z(i)} \quad \textit{Equation 2}$$

Furthermore, the T standard deviation over the levels in a 30 m depth distance under the current level (the current level also included) is express as sigma 30 (σ_{30}). While sigma 10 (σ_{10}) is defined similarly to σ_{30}, but for deeper 10 m depth distance. The σ_{30} and the σ_{10} characterize the consistency of the profile. When a substantial variability of σ_{30} is present, which surpass 0.02 at any depth, then the profile is used for MLD estimation.

The MATLAB MLD script (Appendix 4) was applied (Lorbacher et al., 2006) to the CTD data collected along the transect on the base of potential density, potential temperature and salinity profiles (Figure 8). The three estimation of MLD were then averaged and only one mean MLD value was then used for each station for further analysis. For this region, the MLD was calculated below 10 m depth, to avoid the noisy surface data (see Appendix 4). The selection of the depth (10 m) was based on the slope observed on single station profiles for each cruise.

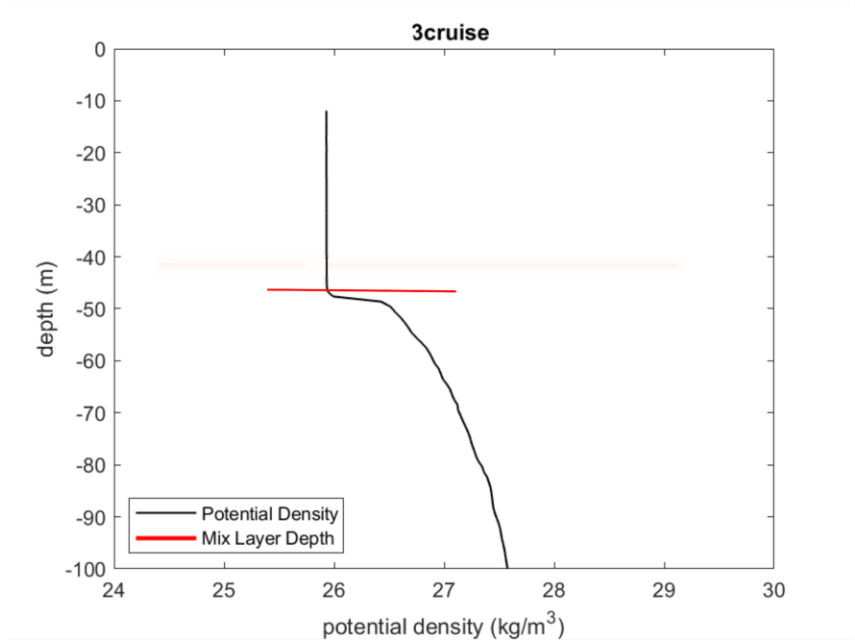

Figure 8. MATLAB Lorbacher et al. (2006) script output for station 5 of Cruise 3 using potential density (Appendix 4).

3.3. Determination of the depth of the DCM

One of the most distinctive structures of the phytoplankton displacement in the MS is the incidence of a DCM through an extense period of the year, in which can be noticed a clear stratified water column (Estrada, 1996; Estradal & Marrase, 1987). The occurrence of the DCM emphasizes the strong vertical distinction found in the marine ecosystem, in which is found a nutrient-limited upper layer with enough light availability to sustain primary production (low nutrient concentration relies on recycled production), and a zone where new production takes place with nutrient enough concentrations, but here light is the limiting factor being light-limited lower layer, (Estrada, 1996). The data of in situ vertical fluorescence profiles has been plotted cruise by cruise and using a simple MATLAB script, the level of maximum fluorescence has been defined station by station. As fluorescence from the automatic probe is not calibrated with Chlorophyll samples during the CNR-ISMAR cruise, no units will be given and only the depth of the DCM is considered to be relevant for this thesis research purpose. Figure 9 shows the fluorescence vertical profile of one cruise as an example, in which the blue dashed line indicates the DCM depth.

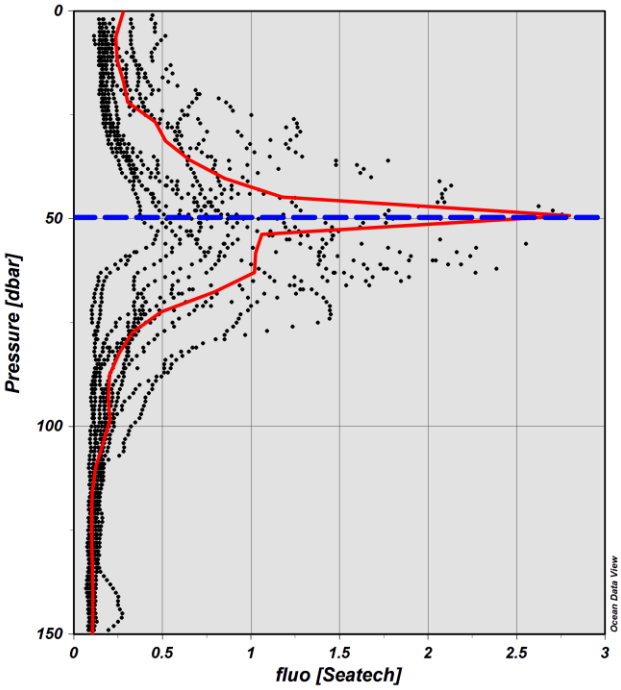

Figure 9. Fluorescence vertical profiles (in black) of all stations along the transect, the red line highlights the station with the deepest DCM, the blue horizontal line highlights the depth to the DCM, where the fluorescence peak is recognized (Cruise 1 – MEDOCC05, May 2005).

3.4. Determination of nutricline depths

Given that dissolved inorganic nutrient data were measured in about 50 % of all CTD stations, and only at standard depths, in order to have a complete picture of their distribution along the horizontal and the vertical dimension, the biogeochemical data have been interpolated (using a Data-Interpolating Variational Analysis, or DIVA[1], method) along the section, using the software Ocean Data View (ODV[2]). The interpolated fields have then been exported and subsequently uploaded into MATLAB (see Appendix 3), for a more detailed analysis (Figure 10).

A	B	C	D	E	F	G	H	L	T	X	AB	AF	BB	BD	BF
Cruise	Station	Type	yyyy-mm-ddT	Longitude [de	Latitude [deg	Bot. Depth [n	Depth[m]	Temperature[	Salinity[PSU]	Oxygen[ml/l]	Fluorescence	Potential_Ter	SiO2 [ÂµM]	PO4 [ÂµM]	NO3 [ÂµM]
Biofun2010	S2	C	2010-05-10T1	4.60733	39.80367	1297	1.985	16.0141	38.0651	5.63628	0.0753	16.0137	1.34	0.01	0.08
Biofun2010	s16	C	2010-05-11T1	7.39533	39.80333	2769	0.993	17.8439	37.3399	5.3601	0.0366	17.8438	1.03	0.01	0.01
Biofun2010	s18	C	2010-05-11T2	7.81517	39.8035	1656	1.985	17.7812	37.3262	5.37507	0.0492	17.7808	1.12	0.01	0.07
Biofun2010	s19	C	2010-05-12T0	7.9985	39.80317	897	1.985	17.786	37.3738	5.3665	0.0449	17.7857	1.01	0.01	0.01
Biofun2010	s4	C	2010-05-10T1	4.99533	39.80333	2685	1.985	16.1233	38.0999	5.54421	0.0859	16.1229	1.35	0.01	0.01
Biofun2010	S1	B	2010-05-10T1	4.4045	39.80383	106	1.985	16.7665	37.9886	5.45771	0.0328	16.7661	1.17	0.01	0.12
Biofun2010	S10	C	2010-05-11T0	6.20117	39.80217	2852	1.985	16.783	37.1396	5.44222	0.0288	16.7827	1.12	0.01	0.07

Figure 10. Extraction of data

The nutrient gradient (Figure 11) is defined as the rate of change of the nutrient in response of the change of the depth. Thus, to find the nutriclines (phosphate and nitrate clines) the vertical gradient of nitrate and phosphate concentration is computed and then the depth of its maximum value is defined, as well as the concentration of the nutrient at that particular depth (see Appendix 1).

[1] https://www.seadatanet.org/Software/DIVA

[2] https://odv.awi.de/

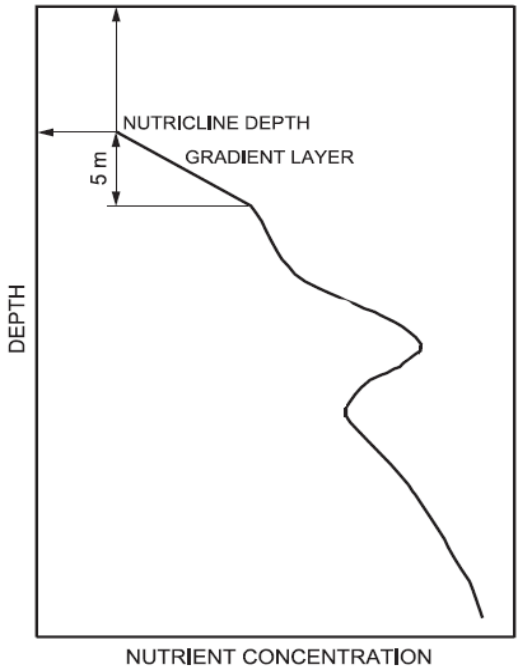

Figure 11. Schematic vertical profile of nutrient concentration with ND and its gradient layer *(Laanemets, 2004)*.

4. Results

In this section for each single cruise the spatial patterns of the nitracline and the phosphacline are shown and then put in relation of the DCM and the MLD patterns.

In the MS, because of its geographical and hydrological characteristics, a strong seasonal signal is well evident. On the Minorca-Sardinia transect it is expected to observe the development of a shallow mixed layer during summer when stratification due to solar heating is maximum, and deep mixed layer during winter when convective processes caused by evaporation, strong winds and strong cooling; these patterns induce seasonal changes in the near-surface circulation (Send et al., 1999). The following figures show only the first few hundred meters, where these interfaces are localized.

4.1. Cruise1 – May 2005 (MEDOCC05)

In spring (May 2005, Figure 12) the nutricline (right) and phosphacline (left) depths (red lines) vary between 40 and 115 m. They reproduce moderate mean concentrations of nitrate along nitracline (~1.93 µmol/kg) and phosphate (~0.14 µmol/kg) along the phosphacline.

Their separation is negligible (on average 0 ±17 m), and both are shallower on the West and deeper on the East, but with a strong shallowing at 7°-7.5°E (probably because of the presence of a cyclonic eddy).

The evolution along the transect of the two nutriclines, the DCM and the MLD (Figure 13) shows the mean MLD at 30 ±6.3 m, the mean DCM depth at 54 ±10 m, the mean nitracline at 65 ±13 m and the mean phosphacline at 65 ±17 m. The difference of MLD and DCM depths is about 20 m, MLD being shallower than the nutriclines and the DCM. Both nutriclines resemble the DCM very much with the exception of the eastern part where DCM goes up and nutricline goes down. The mean nitrate concentration along the DCM was 1.03 ±1.3 µmol/kg and the mean phosphate concentration along DCM was 0.11 ±0.03 µmol/kg. Nitrate concentration at the DCM increase

westwards (from 1 to 3 µmol/kg), while the phosphate concentration increases just at the central-east region of the transect (from 0.13 – 0.16 µmol/kg).

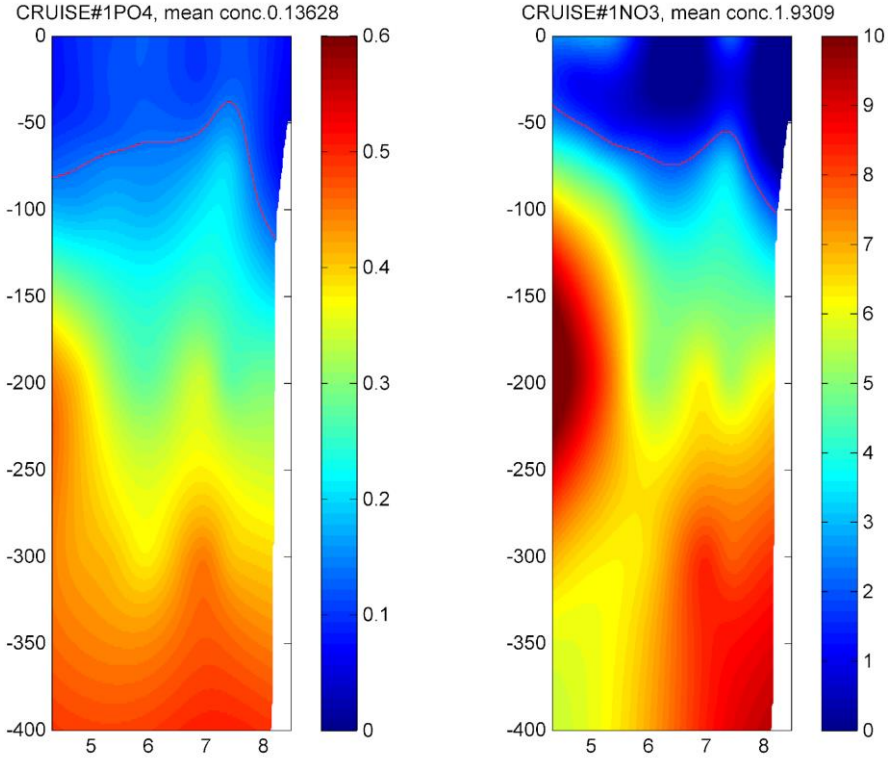

Figure 12. Vertical sections of phosphate and nitrate. The red lines denote the depth of the two nutriclines (Cruise 1, May 2005).

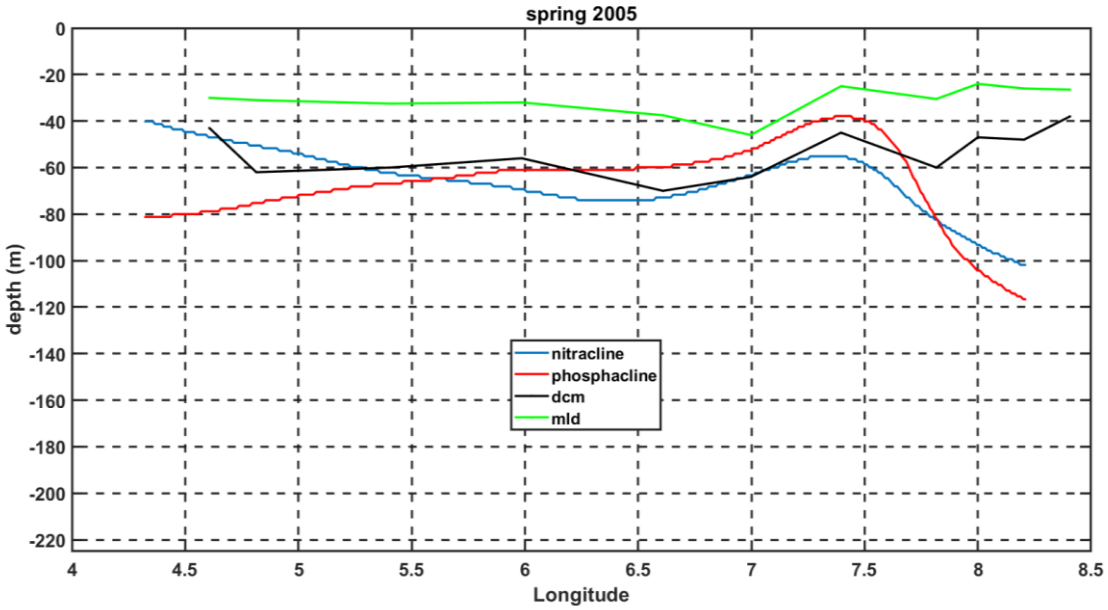

Figure 13. Horizontal distribution of the ND, ML and DCM depths (Cruise 1, May 2005).

4.2. Cruise 2 – June 2006 (Medocc6)

In summer (June 2002, Figure 14) the nutricline (right) and phosphacline (left) depths (red lines) vary between 70 and 120 m. They reproduce high mean concentrations of nitrate along the nitracline (~3.03 µmol/kg) and phosphate (~0.21 µmol/kg) along the phosphacline.

Their separation is negligible (on average 4.35 ±12 m) and both are shallower on the West, and increasing their depth eastwards, with a shallowing of the phosphacline at 5.5°E (short life cyclonic eddy).

The evolution along the transect of the two nutriclines, the DCM and the MLD (Figure 15) shows the mean MLD at 23 ±7.6 m, the mean DCM depth at 66.8 ±12 m, the mean nitracline at 93.7 ±13.4 m and the mean phosphacline at 98 ±18.9 m. The difference of MLD and DCM depths is about 40 m, MLD being shallower but moving up and down following the same pattern of the DCM. Both nutriclines resemble the DCM very much from 4°E to 6.5°E, but from 6.5°E to 8.5°E the nutriclines goes down near 120 m depth and the DCM goes down and up on a range of 40 – 80 m depth.

The mean nitrate concentration along the DCM was 1.6 ±0.5 µmol/kg and the mean phosphate concentration along the DCM was 0.14 ±0.2 µmol/kg. The nitrate concentration at the DCM increase westwards with a low peak at the center of the transect (from 0.9 to 2.3 µmol/kg), while the phosphate concentration increases just at the west of the transect (from 0.11 – 0.16 µmol/kg).

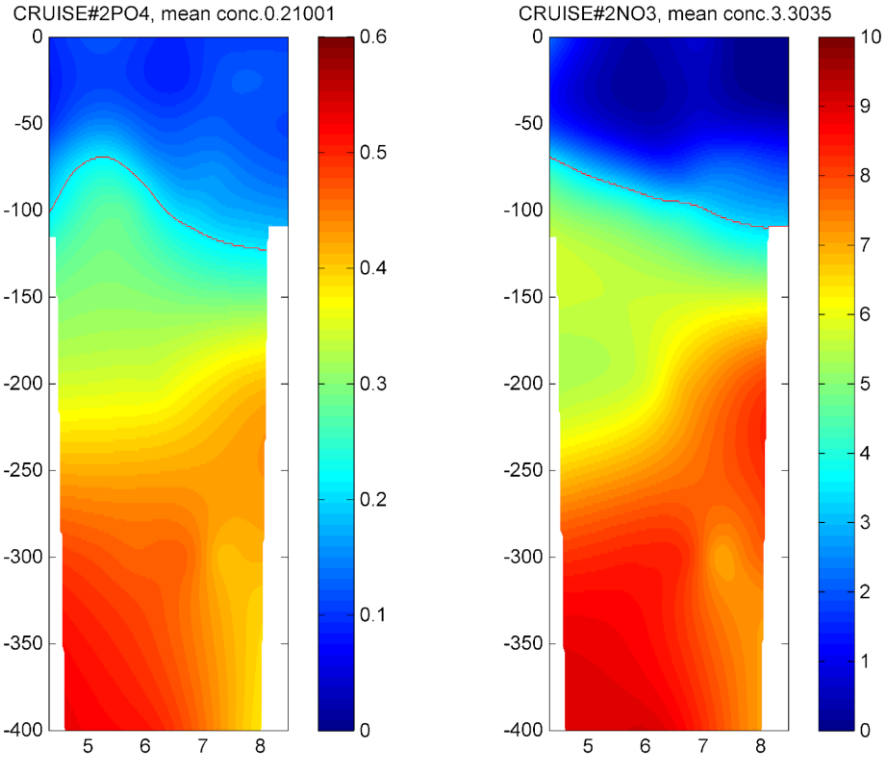

Figure 14. Vertical sections of phosphate and nitrate. The red lines denote the depth of the two nutriclines (Cruise 2, June 2006).

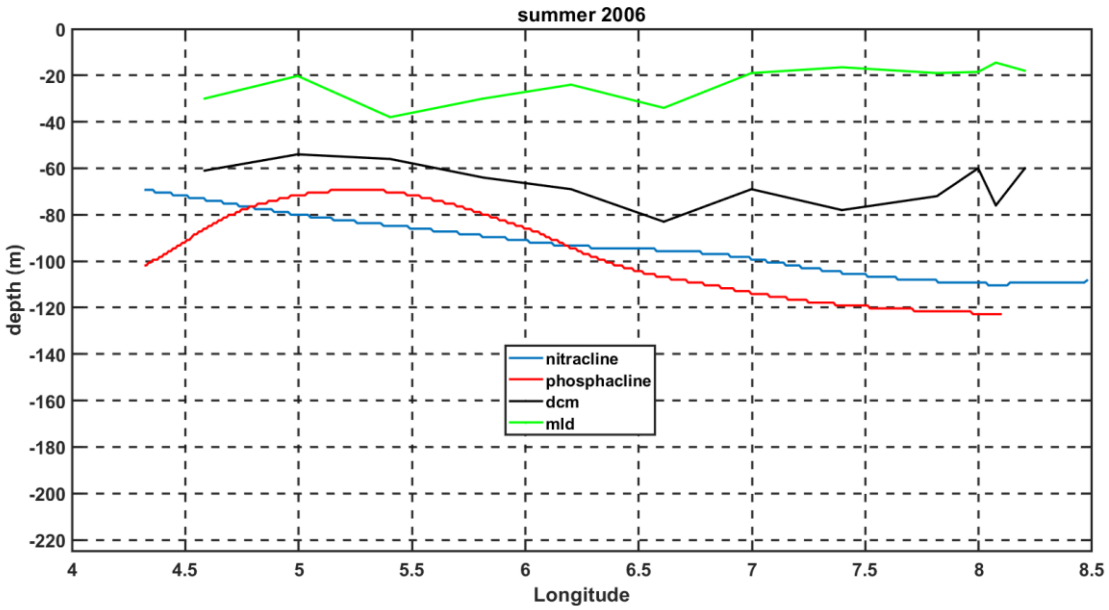

Figure 15. Horizontal distribution of the ND, ML and DCM depths (Cruise 2, June 2006).

4.3. Cruise 3 - October 2007 (MedOcc7)

In autumn (October 2007, Figure 16) the nutricline (right) and phosphacline (left) depths (red lines) vary between 70 and 205 m. They reproduce high mean concentrations of nitrate along nitracline (~3.25 µmol/kg) and phosphate (~0.12 µmol/kg) along the phosphacline.

Their separation is a bit higher, being 18 ± 9 m on average, and both are shallower on the East, deeper at 7°E (long life anticyclonic eddy).

The evolution along the transect of the two nutriclines, the DCM and the MLD (Figure 17) shows the mean MLD at 47±14 m, the mean DCM depth at 69±11 m, the mean nitracline at 135 ±27 m and the mean phosphacline at 153±30.5 m. The difference of MLD and DCM depths is about 20 m, MLD being shallower than the nutriclines and the DCM but moving up and down with their same pattern. Both nutriclines resemble the DCM very much.

The mean nitrate concentration along the DCM was 0.51±0.45 µmol/kg and the mean phosphate concentration along DCM was 0.02±0.1 µmol/kg. The nitrate and phosphate concentrations at the DCM depth both increase eastwards (nitrate from 0.07 to 1.6 µmol/kg, and phosphate from 0.006 to 0.03 µmol/kg)

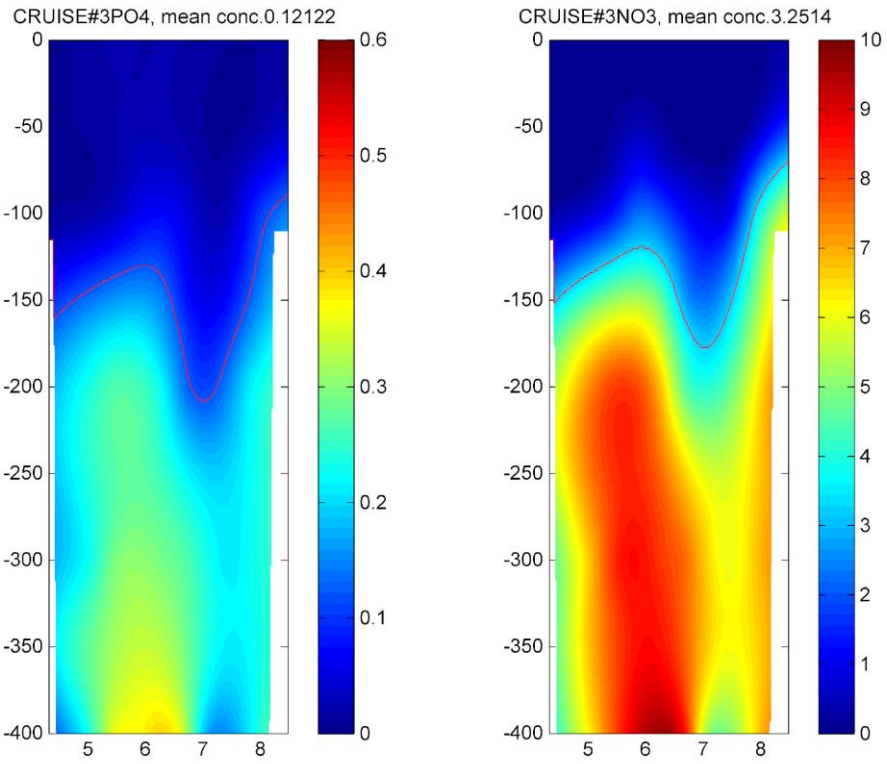

Figure 16. Vertical sections of phosphate and nitrate. The red lines denote the depth of the two nutriclines (Cruise 3, October 2007).

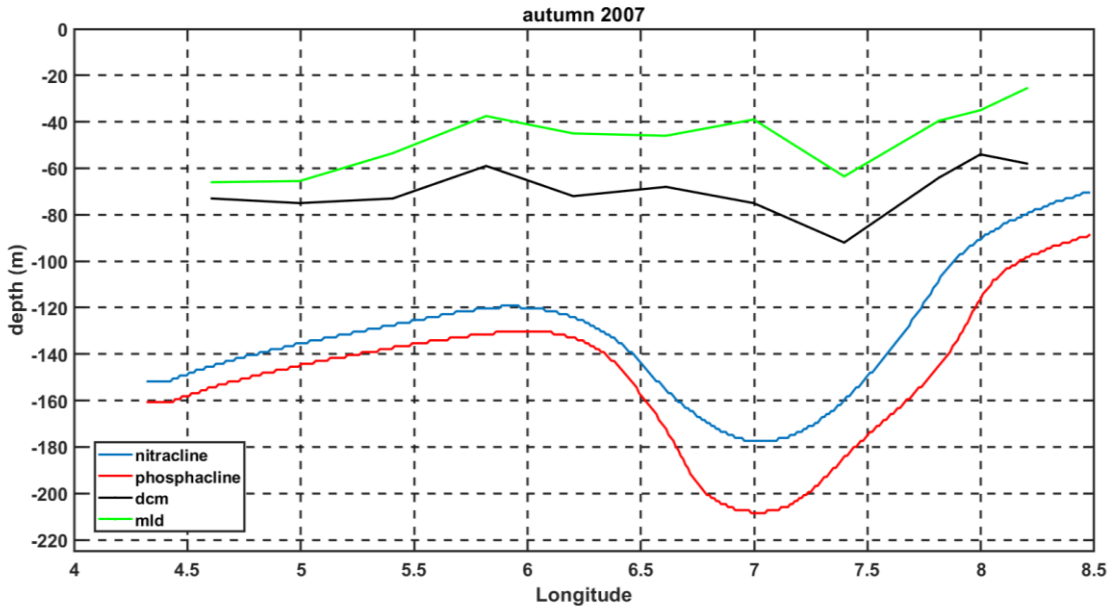

Figure 17. Horizontal distribution of the ND, ML and DCM depths (Cruise 3, October 2007).

4.4. Cruise 4 – May 2010 (Biofun2010)

In spring (May 2010, Figure 18) the nutricline (right) and phosphacline (left) depths (red lines) vary between 132 and 231 m. They reproduce high mean concentrations of nitrate along nitracline (~5.38 µmol/kg) and phosphate (~0.15 µmol/kg) along the phosphacline.

Their separation is negligible (on average 5±8.6 m) and both are shallower on the East and deepens at 6°E (long life anticyclonic eddy).

Both nutriclines resemble the DCM very much, with the exception between 5.5°E to 6.5°E, where the nitraclines reach a deep peak (long life eddy).

The evolution along the transect of the two nutriclines, the DCM and the MLD (Figure 19) shows the mean MLD at 35±11 m, the mean DCM depth at 65±11 m, the mean nitracline at 181±24 m and the mean phosphacline at 186±32 m. The difference of MLD and DCM depths is about 29 m, MLD being shallower than the nutriclines and the DCM. All curves show a deepening between 5.5° and 6.5°E (long life eddy).

The mean nitrate concentration along the DCM was 1.5±0.5 µmol/kg and the mean phosphate concentration along DCM was 0.03±0.007 µmol/kg. The nitrate concentration at the DCM depth increases westwards (from 0.6 to 2.3 µmol/kg), while the phosphate concentration at the DCM depth vary between 0.01 and 0.03 µmol/kg (nearly constant values).

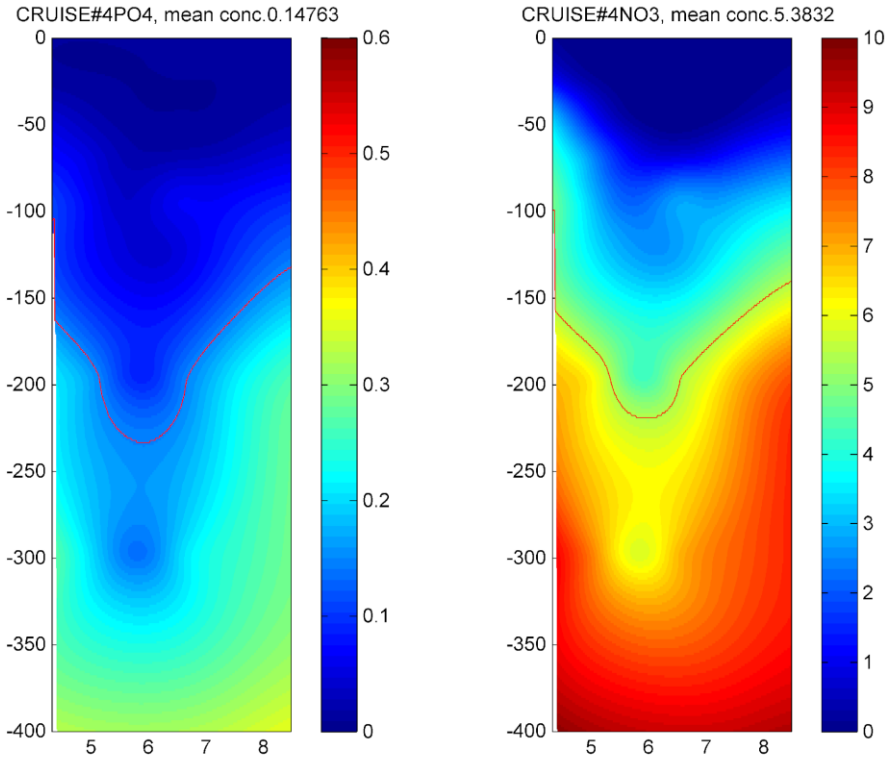

Figure 18. Vertical sections of phosphate and nitrate. The red lines denote the depth of the two nutriclines (Cruise 4, May 2010).

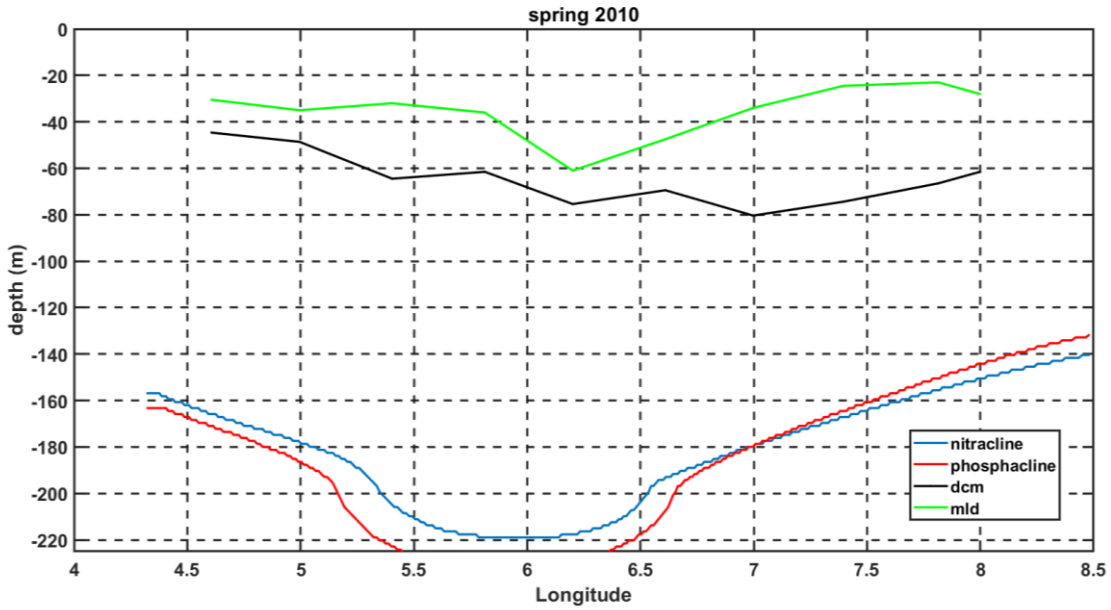

Figure 19. Horizontal distribution of the ND, ML and DCM depths (Cruise 4, May 2010).

4.5. Cruise 5 – November 2011 (Bonifacio2011)

In autumn (November 2011, Figure 20) the nutricline (right) and phosphacline (left) depths (red lines) vary between 70 and 177 m. They reproduce moderate mean concentration of nitrate along the nitracline (~2.66 µmol/kg) and high mean concentration of phosphate (~0.15 µmol/kg) along the phosphacline.

Their separation is significant, being on average 46±5 m, and both are shallower on the West and increasing their depth eastwards.

The evolution along the transect of the two nutriclines, the DCM and the MLD (Figure 21) shows the mean MLD at 49±11 m, the mean DCM depth at 55±12 m, the mean nitracline at 101.27±15 m and the mean phosphacline at 147±14 m. There is almost no separation between MLD and DCM (6 m on average). Both nutricline upwell westwards, while the DCM stays nearly at a constant depth, besides slightly going up eastward with the nutriclines going down.

The mean nitrate concentration along DCM was 0.35±0.5 µmol/kg and the mean phosphate concentration along DCM was 0.014±0.007 µmol/kg. The nitrate concentration at the DCM depth increase westwards (from 0.21 to 1.2 µmol/kg), as well as the phosphate concentration (from 0.005 – 0.02 µmol/kg).

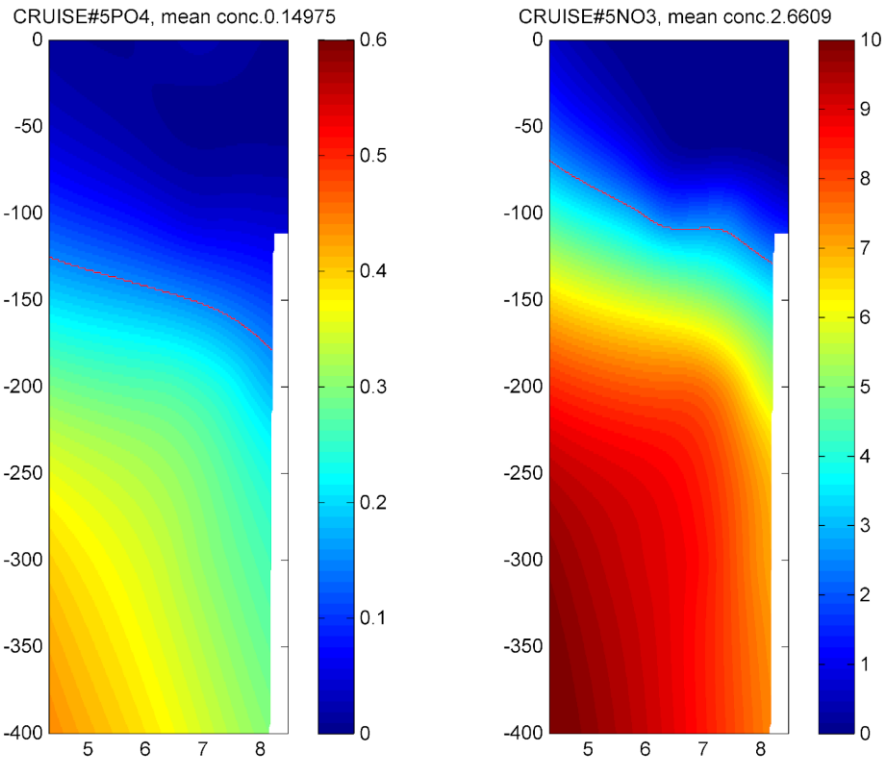

Figure 20. Vertical sections of phosphate and nitrate. The red lines denote the depth of the two nutriclines (Cruise 5, November 2011).

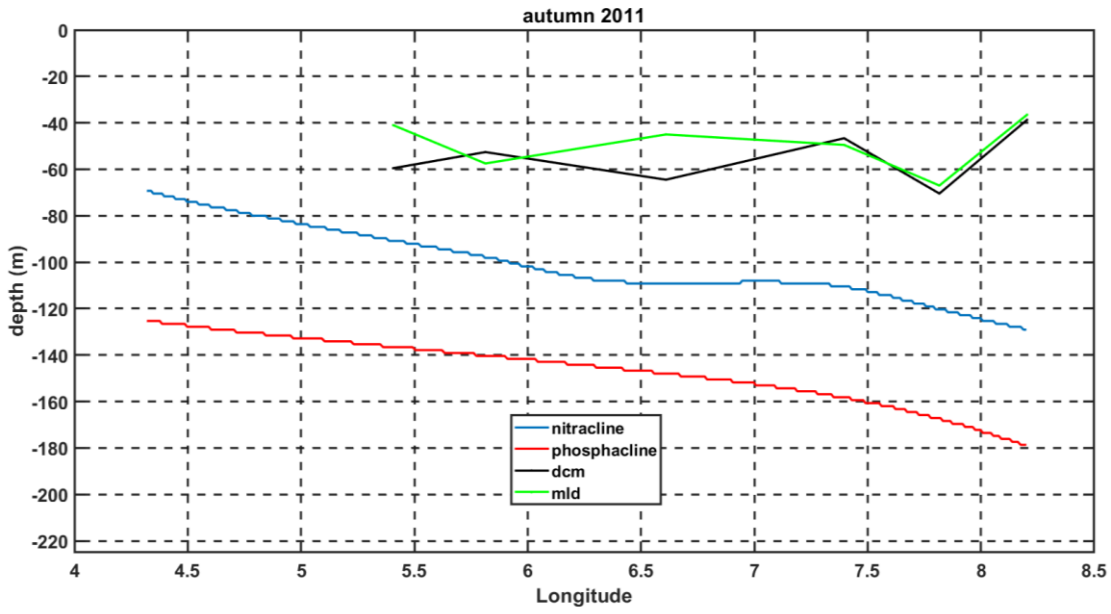

Figure 21. Horizontal distribution of the ND, ML and DCM depths (Cruise 5, November 2011).

4.6. Cruise 6 – January 2012 (Ichnusa 2012)

In winter (January 2012, Figure 22) the nutricline (right) and phosphacline (left) depths (red lines) vary between 50 and 190 m. They reproduce moderate mean concentration of nitrate

along nitracline (~2.31 µmol/kg) and low mean concentration of phosphate (~0.06 µmol/kg) along the phosphacline.

Their separation is very small (7.6±15.9 m on average) and both are shallower on the East and increase their depth westward.

The evolution along the transect of the two nutriclines, the DCM and the MLD (Figure 23) shows the mean MLD at 87±22 m, the mean DCM depth at 27±14 m, the mean nitracline at 110±35 m and the mean phosphacline at 103±47 m. The difference of MLD and DCM depths is about 60 m, MLD being deeper (this is the only cruise where this is observed) and being nearly at the same depth range and with the same pattern as the nutriclines. On the other hand, DCM is very shallow and shows little depth variations, besides going up on the western side with nutriclines going down.

The mean nitrate concentration along the DCM was 0.57±0.75 µmol/kg and the mean phosphate concentration along the DCM was 0.02±0.03 µmol/kg. The nitrate concentration at the DCM depth increase eastwards (from 0.15 to 2 µmol/kg), as well as the phosphate concentration (from 0.001 – 0.04 µmol/kg).

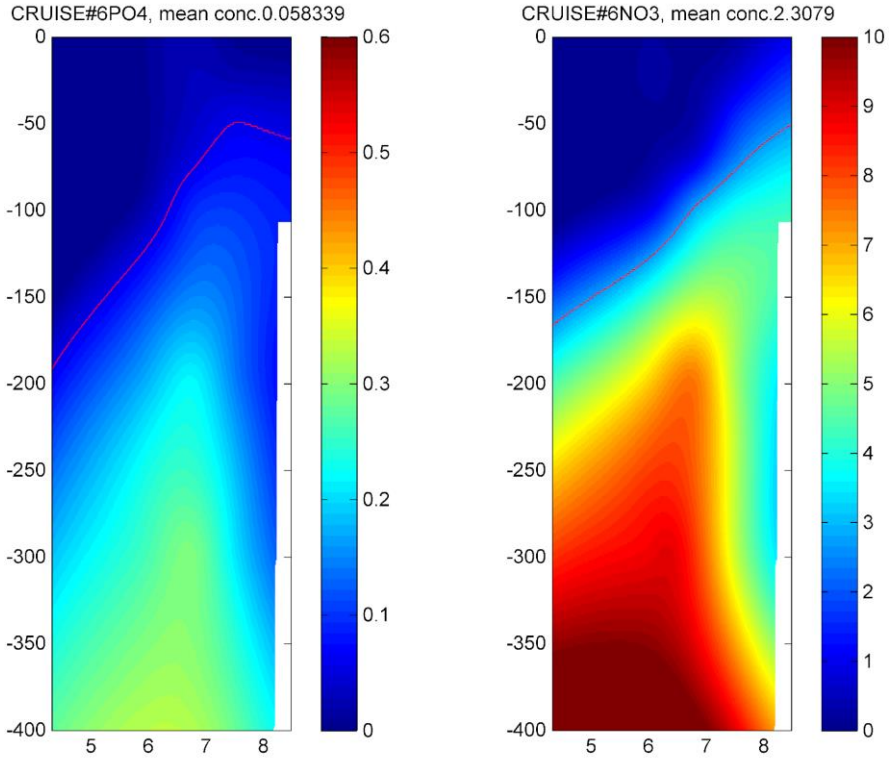

Figure 22. Vertical sections of phosphate and nitrate. The red lines denote the depth of the two nutriclines (Cruise 6, January 2012).

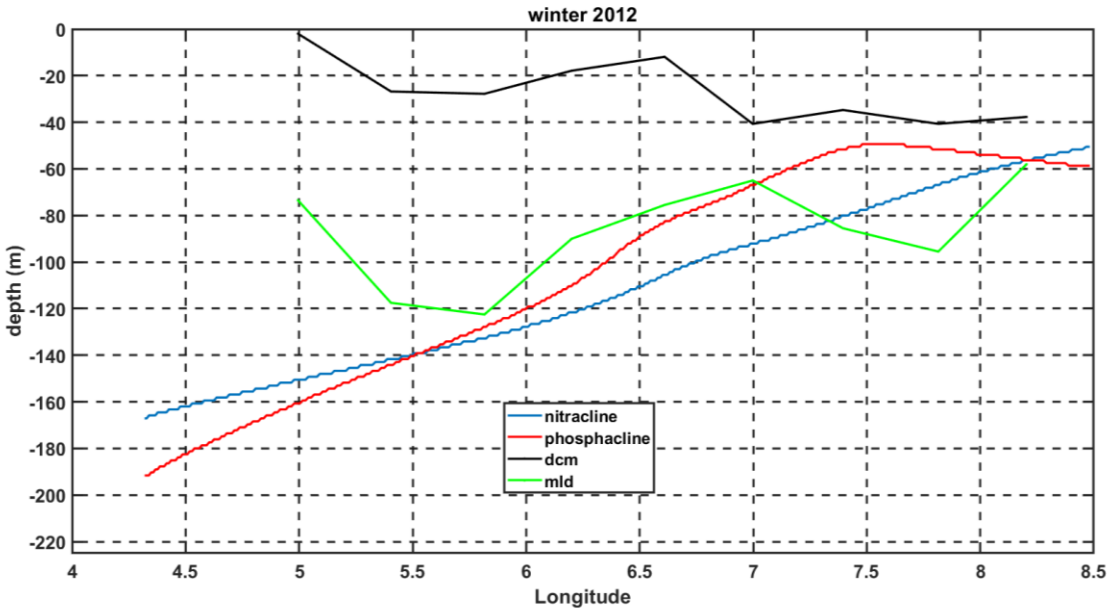

Figure 23. Horizontal distribution of the ND, ML and DCM depths (Cruise 6, January 2012).

4.7. Cruise 7 – August 2015 (Oceancertain_15)

In summer (August 2015, Figure 24) the nutricline (right) and phosphacline (left) depths (red lines) vary between 82 and 160 m. They reproduce moderate mean concentration of nitrate along nitracline (~2.79 µmol/kg) and high mean concentration of phosphate (~0.17 µmol/kg) along the phosphacline.

Their separation is moderate, being on average 30±8 m, and both slightly uplift eastwards.

The evolution along the transect of the two nutriclines, the DCM and the MLD (Figure 25) shows the mean MLD at 20±4 m, the mean DCM depth at 83±11 m, the mean nitracline at 99±9 m and the mean phosphacline at 131±15 m. The difference of MLD and DCM depths is about 60 m, the MLD being shallower and both staying at a nearly constant depth. The DCM stays nearly at the same range of depth of the nitracline.

The mean nitrate concentration along the DCM was 1.72±0.7 µmol/kg and the mean phosphate concentration along DCM was 0.07±0.03 µmol/kg. The nitrate concentration at the DCM depth increase eastwards (from 0.2 to 3 µmol/kg), as well as the phosphate concentration (from 0.01 to 0.1 µmol/kg).

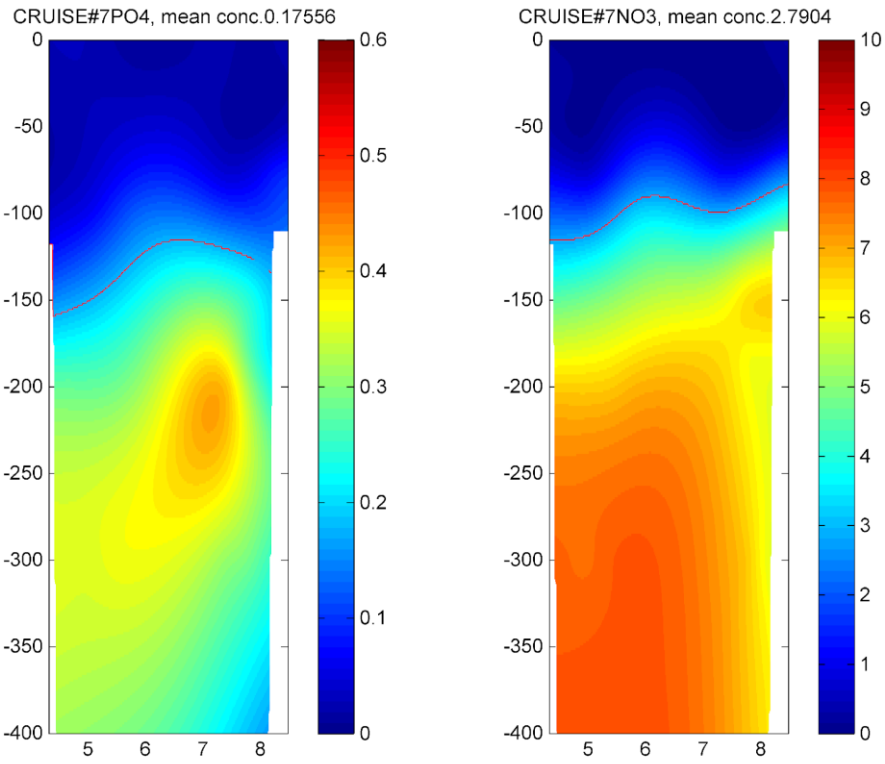

Figure 24. Vertical sections of phosphate and nitrate. The red lines denote the depth of the two nutriclines (Cruise 7, August 2015).

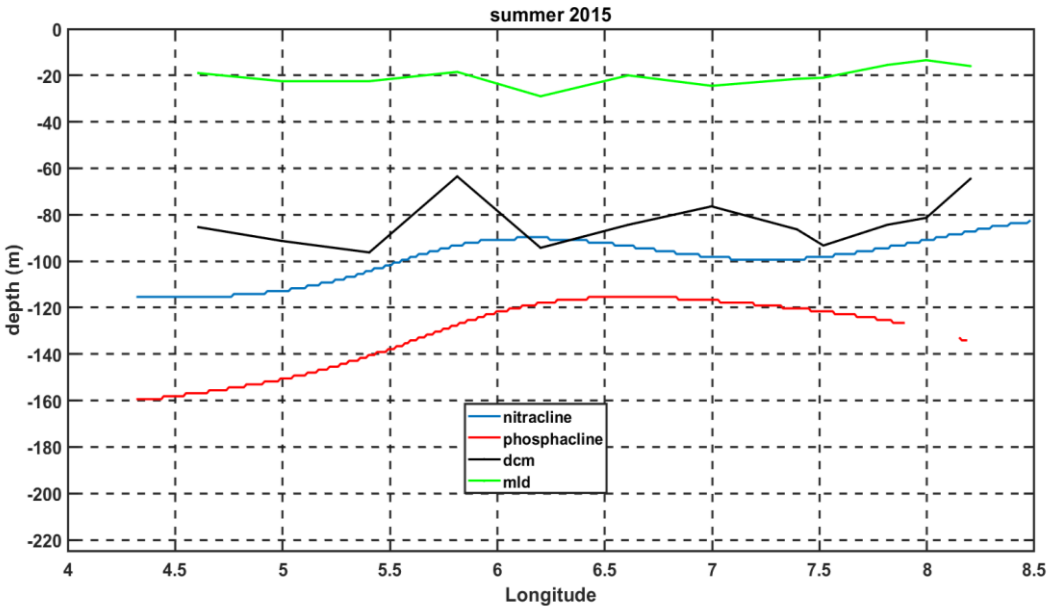

Figure 25. Horizontal distribution of the ND, ML and DCM depths (Cruise 7, August 2015).

5. Discussion

All these interfaces and layers shown in the previous section are also affected by mesoscale dynamics, like passing eddies. To show them more in detail in section 5.1 the thermohaline properties are explored and put in relation to the findings presented in section 4.

During winter, the mixing season, due to the surface buoyancy loss and cooling, the MLD reaches its deepest level (Figure 23) compared to other seasons. At this range vertical mixing generated nitrate and phosphate upwards entrainment into the euphotic layer, enhancing phytoplankton growth. The limiting factor for primary production becomes then light availability, which reduces during winter.

In summer, the stratification season, due to solar heating and less intense air-sea momentum exchanges (due to calm weather), the MLD reaches its shallowest level (Figure 25) compared to other seasons. At this range there is no or very limited upward supply of nutrients and nutriclines remain at a very deep level. The limiting factor for primary production is therefore the nutrient availability, low in summer, rather than light availability, which is usually high in summer. The two extreme cases of summer and winter, described above, well explain the position of the DCM with respect to both the ND and the MLD that were shown in section 4. The other two seasons somewhat represent transition situations. To explore these links more in detail in section 5.2 the primary production is investigated along the transect in different seasons.

5.1. Thermohaline properties along the Minorca – Sardinia transect

On the following figures (26-29) the vertical sections of salinity and potential temperature of the seven cruises (2005, 2006, 2007, 2010, 2011, 2012 and 2015) are shown season by season. During all cruises the Sardinian Vein can be detected along the Sardinian slope, containing Tyrrhenian outflowing water (TDW + LIW), characterized by warm waters and high salinity. These waters (TDW+LIW) can be recognized in the figures by the white thick line on salinity and potential temperature panels. In 2011 (autumn) and 2012 (winter), a thicker Sardinian Vein is observed.

5.1.1. Spring

Figure 26 illustrates the salinity (right) and temperature (left) vertical sections of the Minorca – Sardinia transect in May 2005 - Cruises 1 and in May 2010 – Cruise 4, sampled during spring. Both years show the presence of AW at the surface and warm temperatures at the surface as well. However, there are some noteworthy differences. The AW presence is observed on the surface around 50 m depth in 2005 (salinity ~37.5), while in 2010 the AW near Minorca coast seem to be strongly mixed with warmer and saltier waters (~38 PSU) from below, while in the center of the transect the AW can be observed reaching 200 m of depth in 2010, becoming shallower near the Sardinian shore. This is a typical signature of an anticyclonic eddy crossing the transect, which was well evident also from the ND in Figures 18-19. In 2005 the ND analysis suggested the presence of a cyclonic eddy, which might be the cause of the slight uplifting of the thermocline in the temperature section at 7-7.5°E.

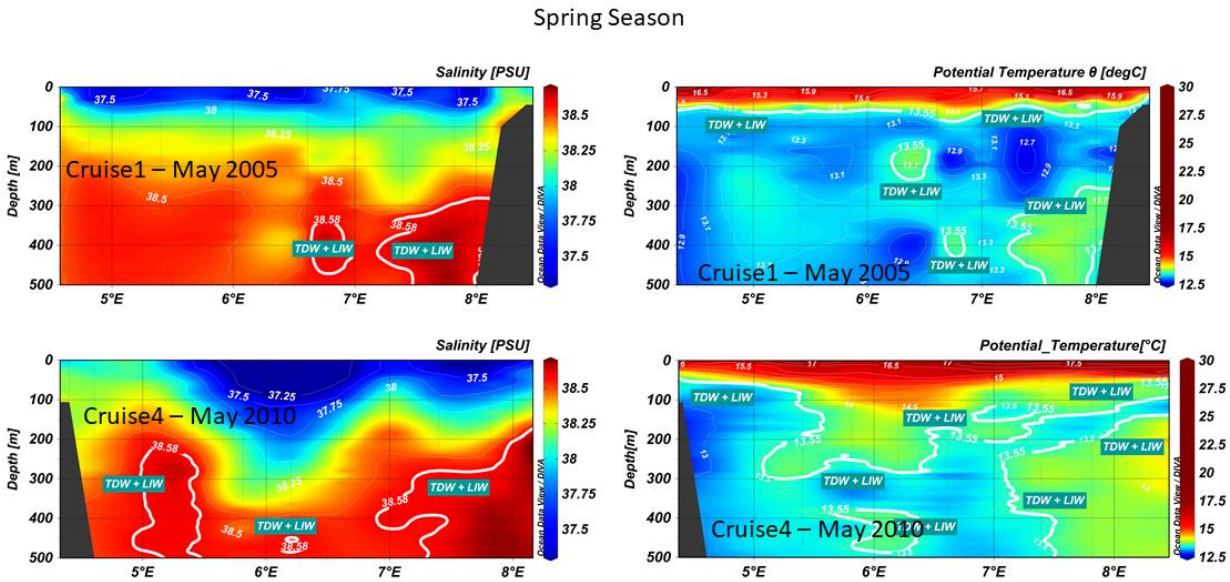

Figure 26. Spring - Zonal sections of salinity (left) and potential temperature (°C) (right).

5.1.2. Summer

Figure 27 illustrates the salinity (right) and temperature (left) vertical sections of the Minorca – Sardinia transect in June 2006 – Cruise 2 and August 2015 – Cruise 7, sampled during summer. The AW water presence is clearer in 2006 within 100 m depth (salinity ~37), while 2015 shows warmer and saltier surface waters, with higher salinity values spread almost up to the top of the water column. In 2006 the presence of an anticyclonic eddy can be recognized, generating a deepening of the isolines at 6°E, which can be also observed from the ND distribution in Figures 14-15. In 2015 a small diameter cyclonic eddy can be recognized, uplifting the isolines, also uplifting ND in Figures 16-17. The MLD reaches its shallowest levels, and nutriclines are found at quite deep levels, hampering the supply of nutrients to the surface layer, and forcing the DCM to stay at depth (Figures 24-25).

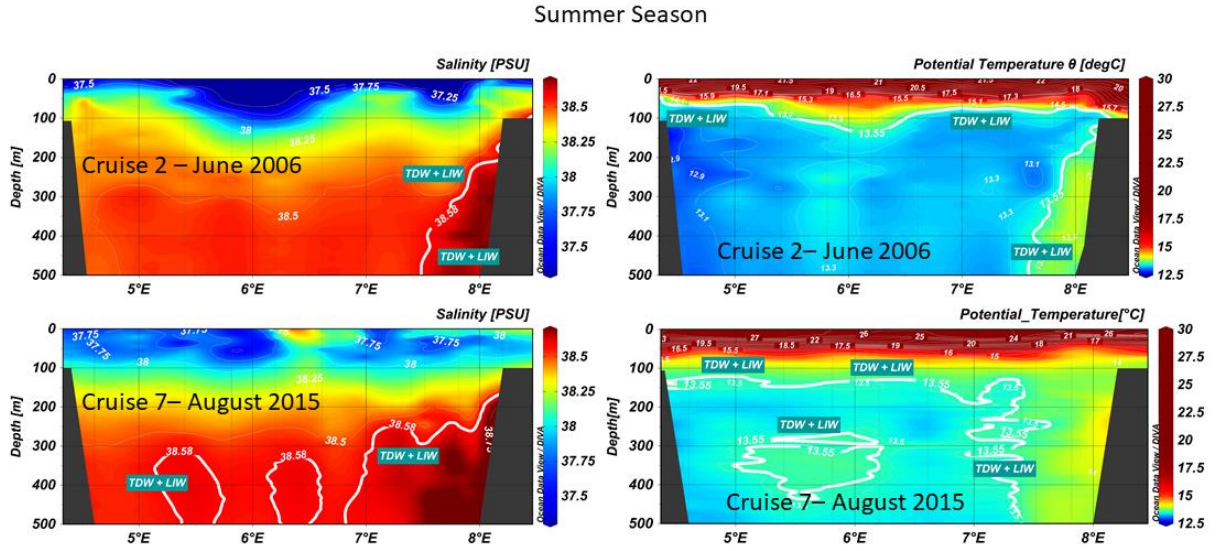

Figure 27. Summer - Zonal sections of salinity (left) and potential temperature (°C) (right).

5.1.3. Autumn

Figure 28 illustrates the salinity (right) and temperature (left) vertical sections of the Minorca – Sardinia transect in October 2007 - Cruise 3 and in November 2011 - Cruise 5, sampled during

autumn. In autumn the sunlight penetration starts to decrease, and the surface water masses start to cool. The presence of mesoscale structures can be observed in 2007, with a deepening of the isolines denoting the interface between AW and LIW at about 7°E, down to 200 m depth. This is a typical signature of an anticyclonic eddy crossing the transect, which was well evident also from the ND distribution in Figures 16-17. A downward displacement of the nutriclines, due to an anticyclone can in fact force the DCM to move downward as well. In 2011, no mesoscale feature has been sampled and the thermohaline properties as well as the nutricline analysis only evidence the presence of the northward flow of the Sardinian Vein.

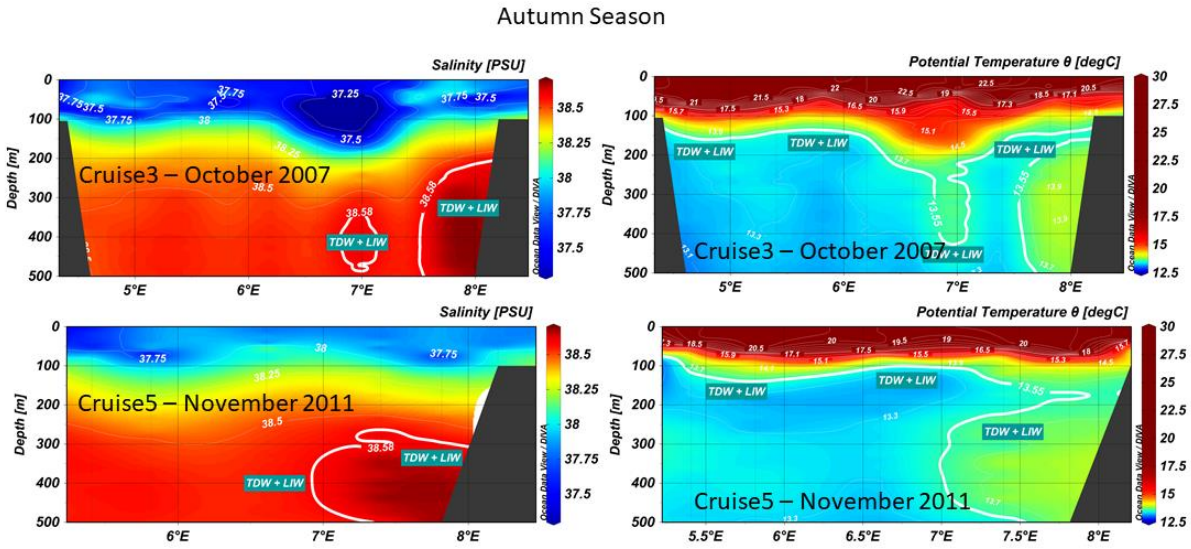

Figure 28. Autumn - Zonal sections of salinity (left) and potential temperature (°C) (right).

5.1.4. Winter

Figure 29 illustrates the salinity (right) and temperature (left) vertical sections of the Minorca – Sardinia transect in January 2012 – Cruise 6, sampled in winter. The temperature and salinity are characterized by strong vertical mixing, and the MLD reaches its deepest level, being deeper on the western side of the transect. This pushes down also the nutriclines, which in fact were 100 m deeper on the western side than on the eastern side (Figure 22-23).

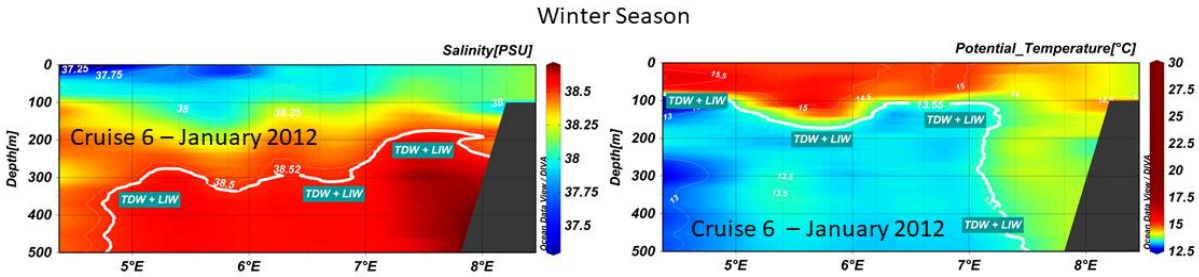

Figure 29. Winter - Zonal sections of salinity (left) and potential temperature (°C) (right).

From the analysis of the thermohaline properties shown in Figure 26 to Figure 29 we found confirmation to Pessini et al. (2018), Testor & Gascard, (2005) and Olita et al., (2013) who described the presence of eddy centers and showed that the mesoscale structures are modes affecting the surface layer over the Minorca – Sardinia transect throughout the year. We have shown how these structures are able to affect the distribution of biogeochemical levels, as the ND and the position of the DCM, with respect to the MLD and the ND. The significance of recognizing these mesoscale structures is the biological response linked with eddies, which is

remarkable and is possible to recognize by ocean colour signatures from satellite images (used as a tracer).

5.2. Primary productivity along the Minorca – Sardinia transect

To understand the seasonal dynamics of the primary production along the investigated transect, vertical sections of the fluorescence measured with a fluorimeter assembled to the CTD are shown in Figure 30 (to be compared with the DCM curves in Figures 13, 15, 17, 19, 21, 23, 25). The depth of the DCM can be clearly identified in its 2D distribution and in different seasons. This gives hints to understand how nutrients and light availability act simultaneously to determine that depth. By comparing cruises of different seasons changes occurring during the stratification season (nutrients sink to deeper layers) and the mixing season (higher nutrient supply to surface layers) can be identified.

Low fluorescence level and a deep DCM is observed during the summer, followed by a slight increase and DCM shallowing in autumn, when the deep chlorophyll layer also becomes thicker. Fluorescence in winter is highest from the surface down to ~150 m depth, before a substantial decrease in intensity and thickness during spring. As the intensity of the fluorescence is particularly high in 2005, we might infer that the samples were taken right after a spring bloom (normally occurring by the end of March). Fluorescence cycle can be linked with a marked interannual variability. In accordance with Volpe et al. (2012) findings, which show a minimum in the chlorophyll amplitude during 1998, maxima decreasing from 1999 to 2004, and exceptional high values during 2005 and 2006, connected to the unusually intense winter convection during 2004/2005.

In summary winter fluorescence enhancement is shown to occur in January 2012 (Cruise 6). Intermittently classical spring bloom regimes were also observed May 2005 (Cruise 1) and in May 2010 (Cruise 4).

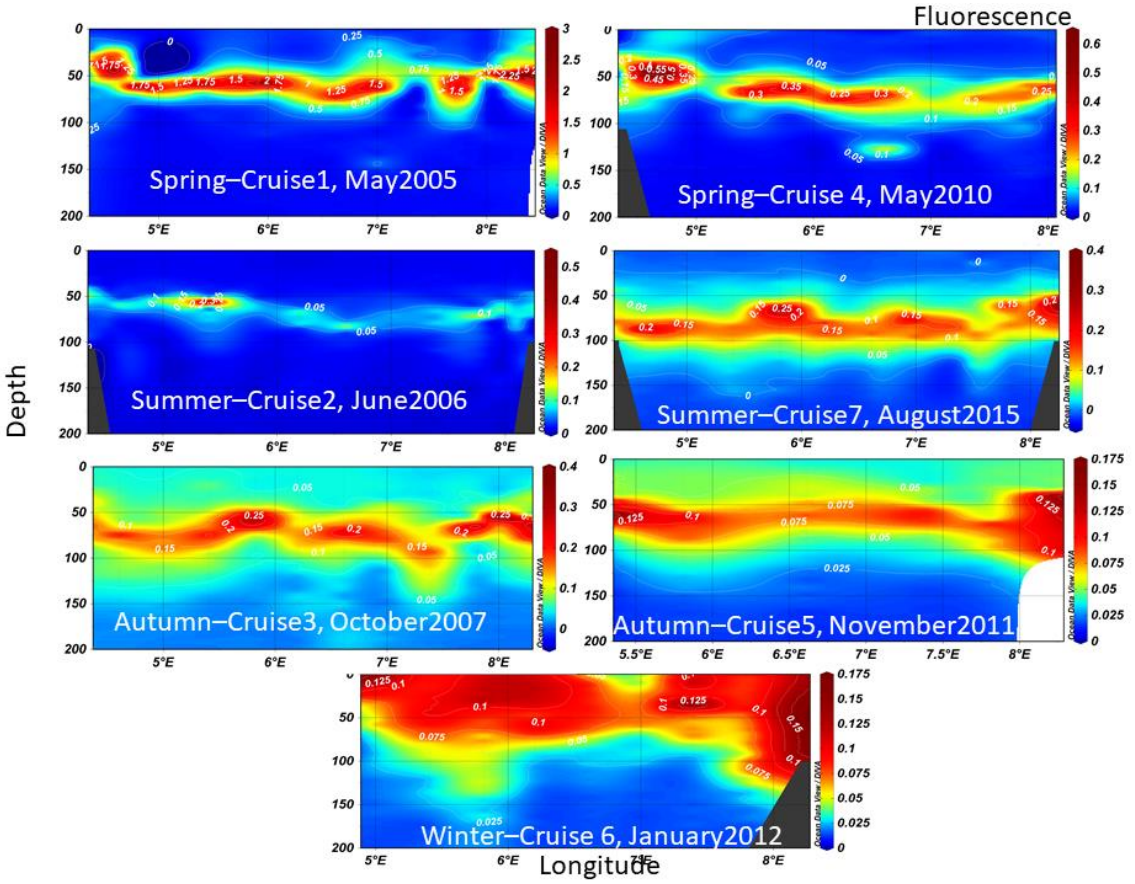

Figure 30. Vertical fluorescence section along the Minorca – Sardinian transect.

5.3. Links between ND, MLD and DCM

The DCM in winter can be recognized at its shallowest depth: affected by low light availability the phytoplankton community stays close to the surface, where due to the strong vertical mixing in winter (deep MLD) they still have enough nutrients supplied from the depth. According to D'Ortenzio (2014), deep MLD events were always concomitant to local decreases of chlorophyll concentrations, as expected during intense mixing episodes. Likewise, Lavigne et al. (2015) have found that the DCM can even disappear in winter. The nutriclines depth more or less resemble the seasonal changes of the MLD (deepest in winter). The MLD deepening coincides with the intensification of local surface winds, probably also favouring the formation of cyclonic and anticyclonic eddies. Nutricline and DCM high separation affect the availability of nutrients to the phytoplankton community, but thanks to the strong effect of vertical mixing the phytoplankton receives a moderate supply of nutrients to keep growing successfully.

Later in spring, due to the surface gradual warming, the water column starts to re-stratify and the MLD is becoming shallower, while phytoplankton activity increases because of an increase in light availability for primary production. The displacement of the DCM in spring can be recognized at moderate depths and the phytoplankton community, affected by moderate light availability, stays at moderate depths, where the optimal growth conditions are found. The availability of nutrients at the DCM are 1.03±1.3 µmol/kg for nitrate and 0.11±0.03 µmol/kg for phosphate. Nutrient content was moderate at the DCM depth for both years, and what is observed is the post spring bloom with high fluorescence values (Figure 26, Figure 30), because the normal bloom period in this region ranges from February to March as reported by D'Ortenzio & D'Alcalà, (2009). The higher nutrient concentration at the DCM depth due to a shallow

nutricline, could be ascribed to a previous strong winter deep convection (i.e. 2004/2005, Schroeder et al., 2016), which brings nutrient from deeper depths to the enlightened surface layer (nutrients concentration at the nutriclines depths were lower in 2005 than in 2010, probably because they were transported to the surface). After the spring blooms, as stratification becomes stronger, surface water masses are characterized by a progressive return to a summer oligotrophy (Mayot et al., 2017). Moreover, the shallowing of the nutriclines observed at 7°E in 2005, may be due to the presence of eddies reported by Béranger et al., (2005) and Olita et al., (2013). Nutriclines were observed at shallowest depths (40 - 115 m) in spring 2005 being shallower on the West, but with a shallowing at 7°-7.5°E probably because of the presence of a mesoscale structure. Contrastingly in 2010 deepest nutriclines depths (132 - 231 m) were observed, being shallower on the East, but with a deepening at 7°E, probably due to a long life anti-cyclonic eddy pushing the layer to deeper depths, as reported by Pessini et al. (2018).

In summer, due to the surface stable buoyancy and warmer temperatures, the MLD reaches its shallowest level at 23±8 m in 2006 and 20±4 m in 2015, being the only period of the year where the MLD is found several tens of meters above the DCM. Light is available at deeper depths, as a result of the concomitant action of the increase in surface sunlight intensity and decreased turbulence (Mignot et al., 2014). Because of sunlight availability and the thickening of the photic layer, the deepest DCM can be observed in this season, associated with higher nutrient concentrations at the same depth. This increased nutrient availability favors the growth of phytoplankton at the DCM (Estrada, 1996): the nutrient concentration at the DCM is 1.6±0.5 µmol/kg (2006) and 1.72±0.7 µmol/kg (2015) for nitrate and 0.14±0.2 µmol/kg (2006) and 0.07±0.03 µmol/kg (2015) for phosphate. In 2006, the DCM is observed at shallower depths (67±12 m) than in 2015 (83.42±10.71 m), the nutriclines being as well shallower in 2006 than in 2015, increasing its depth eastwards in 2006, and westwards in 2015. These differences could be due the intense variability of the region reported by Volpe et al., (2012). Nutriclines were observed at intermediate depths (69.28 - 122 m) in 2006 and in 2015 (82.41 - 159.42 m). In 2006 a shallowing of the phosphacline is observed at 5°E, probably by the presence of eddies (i.e. short and long life described by Pessini et al., 2018). Nutricline mean depth and the mean MLD were separated from each other by 87 m (2006) and 78 m (2015), where the MLD for both years was found at its shallowest level. In 2015, nutriclines were deep (99±9 m mean depth) and were coupled with the DCM (83±11 m mean depth), this short distance might be the reason why higher nutrient concentrations at DCM where found in 2015 than in 2006. Furthermore, the higher separation between DCM and nutriclines (30 m) in 2006 can be the reason why the nutrient concentration at the DCM is lower in 2006 than in 2015.

In autumn, the MLD progressively deepens: in both years that were sampled during autumn, the mean MLD was at 45-50 m depth. In this period of the year sunlight start to decrease as well as the temperature. Also, buoyancy fluxes associated with severe atmospheric events are expected during autumn, coinciding with Volpe et al., (2012) observations. The presence of the DCM in autumn can be recognized by its moderate depth, and the phytoplankton community, affected by decrease in light availability, stays at moderate depths, with the availability of nutrient at the DCM being 0.51±0.45 µmol/kg (2007) and 0.35±0.5 µmol/kg (2011) for nitrate and 0.02±0.1 µmol/kg (2007) and 0.014±0.007 µmol/kg (2011) for phosphate. The previous nutrient values at the DCM coincide with Lavigne, (2015) reports, who conclude that the DCM is ubiquitous in this season. A DCM displacement to shallower depths was noticed (mainly because of the sunlight intensity decrease), following the nutricline and MLD (forming parallel lines). In 2011 a shallowing (deepening) of the DCM (nutriclines) is observed from 8°E to the east,

probably because of the presence of eddies. The nutricline deepening in 2007 coincides with mesoscale structures reported in the area. Nutricline mean depth and the mean MLD were separated from each other by 93 m (2007) and 50 m (2015). The nutriclines depth coincide with the MLD deepening and were observed at a deeper depth in October 2007 (70 - 205 m) than in November 2011 (69- 177 m).

6. Conclusions and recommendations

This thesis research gives the opportunity to investigate the ND, MLD and DCM dynamics variability in the Minorca – Sardinia transect between 2005 and 2015. The simultaneous availability of thermohaline properties, dissolved NO_3, dissolved PO_4 and fluorescence in situ data allow a unique reconstruction of the physical, biogeochemical interactions in the APB. The study has been realized with the aim to analyze possible links between the temporal and spatial dynamics of the ND depth with the controlling factors MLD and DCM depth. The Minorca-Sardinia transect is in a transition region between two different dynamic regimes: the AB (region dominated by mesoscale baroclinic instability) and the PB (the region of dense water mass formation and general cyclonic boundary circulation), for this reason the nutriclines (phosphacline and nitracline), DCM and MLD present a wide range of variable depths (deepening or shallowing in specific longitudes), than in other regions of the WMED.

The Minorca -Sardinia transect is a moderate productive area of the open sea region of the WMED basin and can be considered as a mesothrophic region. However, during early spring, especially after strong winter induced convention events, the transect region can become more productive, showing interannual or intermittent spring blooms. This production is essentially based on new production, due to the vertical import of high nutrients levels into the surface layer during deep convection and violent mixing in general. Moreover, spring is the most variable season, showing a very shallow nutricline in 2005 and a deep one in 2010, as an effect of a strong vertical mixing convention during the previous winter (2005) or after a mild vertical mixing during the previous winter (2015), respectively.

As expected, the Minorca - Sardinia transect shows a strong seasonal variability of the MLD, which is affected by thermal stratification during summer and mixing convection during winter. A shallower MLD in summer, with less dense and warmer surface waters, is linked with a deepening of the nutricline, which in turn affects the nutrient supply to the euphotic layers and consequently the DCM is less intense and deepens, therein declining the primary productivity. This pattern was particularly evident in summer 2006 and 2015. The DCM depth interannual variability seems to be strongly linked with the ND and consequently by the separation between nitracline and phosphacline.

Concerning the DCM dynamics in the Minorca – Sardinia transect, the results obtained agrees with what was found by García-martínez et al. (2018) and Estrada (1996), i.e. that maxima DCM can be observed after winters as a consequence of strong convention events (as in 2004/2005). The results obtained for the fluorescence levels in this thesis research are in good agreement with Volpe et al. (2012), who concluded that the phytoplankton dynamics in certain regions of the WMED can present interannual variability (Figure 30). Besides Cermeno et al. (2008) highlighted the implication of stronger thermal stratification periods over the productivity of the primary production (inverse relation), therein affecting the carbon capture capacity of the oceans (carbon pump), by an equilibrium of the phytoplankton taxa. Conclusively, the findings

on DCM dynamics results coincide with Lavigne (2015) and Volpe et al (2012) reports, which conclude that DCM is generally higher during spring and summer.

For spring, the findings agree with Béranger et al., (2005), who report the presence of the long-life anticyclonic eddies (during April to June). The nutriclines depth coincide with the MLD deepening. The autumn cruises seem to be affected by the presence of an anti-cyclonic mesoscale structures, observed by a deepening of the nutriclines, as well as the DCM and MLD.

There are several areas of this thesis that can be researched further. One is to apply the methodology of analysis of ND temporal and spatial dynamics over different transects along the different basins of the MS (i.e. Tyrrhenian Sea, Provençal Basin, Gulf of Lions, etc.). A wide area of sampling has provided a robust database (Belgacem et al., in preparation), which will allow to have a better view of the ND temporal and spatial dynamics.

A limitation of the present research thesis is that the database does not have a complete daily or monthly or yearly samples (i.e., entire month of year). For this reason, the analysis of this transect of the following months: February, March, April, July, September, and November would complete the overview of the nutrients dynamics of the transect. More data are required to improve the understanding of phytoplankton dynamics and its link with the ND temporal and spatial variability. Also, analyzing more in detail the effect of coupling or decoupling between the nitracline and the phosphacline would represent a noteworthy follow up of this study.

Another area that can be further explored for a better understanding of the ND dynamics is the one exposed by Urtizberea et al. (2013) where the 'Coloured dissolved organic matter' (CDOM) has been analyzed as an important component of the background light attenuation, which affects the phytoplankton nutrient consumption, which should be investigated in more detail. The variation in CDOM attenuation can affect basic properties of the euphotic zone in the common marine ecosystem model. According to Longhurst (2006) the analysis of the iron in water sample can also give a deeper understanding of the interaction between the nutricline and the phytoplankton consumption.

It would also be worth looking at some higher detail of analysis the coalescence processes and merging of the Sardinian eddies documented by Testor & Gascard (2005), in the Minorca and Sardinia transect, where an accumulation of these eddies can occur and as has been observed in the present analysis can modify the ND expected seasonality.

Finally, it would be interesting to compare the Minorca – Sardinian transect with the other oceanic regions, following D'Ortenzio & D'Alcalà, (2009), which reports that the Mediterranean basin present the same "mixture" of trophic regimes as the North Atlantic ocean regions (meridional physical boundary of the North Atlantic bloom is usually localized at 35 - 40°N), enclosed in a restricted latitudinal extension (30 –43°N). The authors follow Longhurst (1995) model, supporting the fact that temporal dynamics are analogous, but the Mediterranean pattern fluctuate in time (or in latitude) in comparison with the corresponding regions in the North Atlantic.

In general, ND variability during the 2005 – 2015 period, obtained in the present work can be used as a reference for future works or operational services providing reference values and ranges.

References

Beckmann, A., & Hense, I. (2007). Beneath the surface: Characteristics of oceanic ecosystems under weak mixing conditions - A theoretical investigation. Progress in Oceanography, 75(4), 771–796. https://doi.org/10.1016/j.pocean.2007.09.002

Belgacem M., Chiggiato J., Borghini M., Pavoni B., Cerrati G., Acri F., S. Cozzi, M. Alvarèz, Schroeder K. Dissolved Inorganic Nutrients in the Western Mediterranean Sea (2004-2017), in preparation for ESSD, 2019.

Béranger, K., Mortier, L., & Crépon, M. (2005). Seasonal variability of water transport through the Straits of Gibraltar, Sicily and Corsica, derived from a high-resolution model of the Mediterranean circulation. Progress in Oceanography, 66(2–4), 341–364. https://doi.org/10.1016/j.pocean.2004.07.013

Béthoux, J. P., Morin, P., Chaumery, C., Connan, O., Gentili, B., & Ruiz-Pino, D. (1998). Nutrients in the Mediterranean Sea, mass balance and statistical analysis of concentrations with respect to environmental change. *Marine Chemistry*, *63*(1-2), 155-169.

Béthoux, J. P. (1979). Budgets of the Mediterranean Sea-Their dependance on the local climate and on the characteristics of the Atlantic waters. Oceanologica Acta, 2(2), 157–163.

Bethoux, J. P., Gentili, B., Morin, P., Nicolas, E., Pierre, C., & Ruiz-Pino, D. (1999). The Mediterranean Sea: A miniature ocean for climatic and environmental studies and a key for the climatic functioning of the North Atlantic. Progress in Oceanography, 44(1-3), 131-146. https://doi.org/10.1016/S0079-6611(99)00023-3

Bryden, H. L., Candela, J., & Kinder, T. H. (1994). Exchange through the Strait of Gibraltar. Progress in Oceanography, 33(3), 201–248. https://doi.org/10.1016/0079-6611(94)90028-0

Catalá, T. S., Martínez-Pérez, A. M., Nieto-Cid, M., Álvarez, M., Otero, J., Emelianov, M., … Álvarez-Salgado, X. A. (2018). Dissolved Organic Matter (DOM) in the open Mediterranean Sea. I. Basin–wide distribution and drivers of chromophoric DOM. Progress in Oceanography, 165, 35–51. https://doi.org/10.1016/j.pocean.2018.05.002

Cermeno, P., Dutkiewicz, S., Harris, R. P., Follows, M., Schofield, O., & Falkowski, P. G. (2008). The role of nutricline depth in regulating the ocean carbon cycle. Proceedings of the National Academy of Sciences, 105(51), 20344–20349. https://doi.org/10.1073/pnas.0811302106

Champalbert, G. (1996). Characteristics of zooplankton standing stock and communities in the Western Mediterranean Sea: Relations to hydrology. Scientia Marina, 60(2), 97–113.

Cullen, J. J. (1982). The deep chlorophyll maximum: comparing vertical profiles of chlorophyll a. Canadian Journal of Fisheries and Aquatic Sciences, 39(5), 791-803.

D'Ortenzio, F., & Ribera d'Alcala, M. (2009). On the trophic regimes of the Mediterranean Sea: A satellite analysis. Biogeosciences, 6, 139–148.

D'Ortenzio, F., Lavigne, H., Besson, F., Claustre, H., Coppola, L., Garcia, N., ... & Morin, P. (2014). Observing mixed layer depth, nitrate and chlorophyll concentrations in the northwestern Mediterranean: A combined satellite and NO3 profiling floats experiment. Geophysical Research Letters, 41(18), 6443-6451. https://doi.org/10.1002/2014GL061020

Estrada, M. (1996). Primary production in the northwestern Mediterranean. Scientia Marina, 60(Supl. 2), 55–64.

Estrada, M., Marrasé, C., Latasa, M., Berdalet, E., Delgado, M., & Riera, T. (1993). Variability of deep chlorophyll maximum characteristics in the Northwestern Mediterranean. Marine Ecology Progress Series, 289-300.

Fine, E. C., Bryan, F. O., Large, W. G., & Bailey, D. A. (2015). An initial estimate of the global distribution of diurnal variation in sea surface salinity. *Journal of Geophysical Research: Oceans*, *120*(5), 3211-3228.

Fuda, J. L., Millot, C., Taupier-Letage, I., Send, U., & Bocognano, J. M. (2000). XBT monitoring of a meridian section across the western Mediterranean Sea. *Deep Sea Research Part I: Oceanographic Research Papers*, *47*(11), 2191-2218.

García-Martínez, C., Vargas-yáñez, M., Moya, F., Santiago, R., Muñoz, M., Reul, A., … Balbín, R. (2018). Average nutrient and chlorophyll distributions in the Western Mediterranean: RADMED project. Oceanologia. https://doi.org/10.1016/j.oceano.2018.08.003

García, M. J., Millot, C., Font, J., & García-Ladona, E. (1994). Surface circulation variability in the Balearic Basin. Journal of Geophysical Research: Oceans, 99(C2), 3285-3296. https://doi.org/10.1029/93JC02114

Garcia, N., Raimbault, P., Gouze, E., & Sandroni, V. (2006). Nitrogen fixation and primary production in Western Mediterranean. Comptes Rendus - Biologies, 329(9), 742–750. https://doi.org/10.1016/j.crvi.2006.06.006

Gómez-Navarro, L., Fablet, R., Mason, E., Pascual, A., Mourre, B., Cosme, E., & Le Sommer, J. (2018). SWOT Spatial Scales in the Western Mediterranean Sea Derived from Pseudo-Observations and an Ad Hoc Filtering. Remote Sensing, 10(4), 599. https://doi.org/10.3390/rs10040599

Grasshoff, K., Kremling, K., Ehrhardt, M. (1999). Methods of Seawater Analysis. Wiley-Vch Verlag, Weinheim, Germany.

Hanson, C. E., Pesant, S., Waite, A. M., & Pattiaratchi, C. B. (2007). Assessing the magnitude and significance of deep chlorophyll maxima of the coastal eastern Indian Ocean. Deep-Sea Research Part II: Topical Studies in Oceanography, 54(8–10), 884–901. https://doi.org/10.1016/j.dsr2.2006.08.021

Houpert, L., Testor, P., de Madron, X. D., Somot, S., D'Ortenzio, F., Estournel, C., & Lavigne, H. (2015). Seasonal cycle of the mixed layer, the seasonal thermocline and the upper-ocean heat storage rate in the Mediterranean Sea derived from observations. Progress in Oceanography, 132, 333–352. https://doi.org/10.1016/j.pocean.2014.11.004

Huthnance, J. M., Coelho, H., Griffiths, C. R., Knight, P. J., Rees, A. P., Sinha, B., … Chatwin, P. G. (2001). Physical structures, advection and mixing in the region of Goban spur. Deep-Sea Research Part II: Topical Studies in Oceanography, 48(14–15), 2979–3021. https://doi.org/10.1016/S0967-0645(01)00030-3

Ouellet Jobin, V., & Beisner, B. E. (2014). Deep chlorophyll maxima, spatial overlap and diversity in phytoplankton exposed to experimentally altered thermal stratification. Journal of Plankton Research, 36(4), 933-942. https://doi.org/10.1093/plankt/fbu036

Kara, A. B., Rochford, P. A., & Hurlburt, H. E. (2000). An optimal definition for ocean mixed layer depth. Journal of Geophysical Research: Oceans, 105(C7), 16803-16821. https://doi.org/10.1029/2000JC900072

Karimova, S. (2018). Eddies in the Western Mediterranean seen in thermal infrared imagery and SLA fields. International Journal of Remote Sensing, 39(13), 4304–4329. https://doi.org/10.1080/01431161.2018.1454626

Klein, B., Roether, W., Manca, B. B., Bregant, D., Beitzel, V., Kovacevic, V., & Luchetta, A. (1999). The large deep water transient in the Eastern Mediterranean. Deep-Sea Research Part I: Oceanographic Research Papers, 46(3), 371–414. https://doi.org/10.1016/S0967-0637(98)00075-2

Kress, N., & Herut, B. (2001). Spatial and seasonal evolution of dissolved oxygen and nutrients in the Southern Levantine Basin (Eastern Mediterranean Sea): chemical characterization of the water masses and inferences on the N: P ratios. Deep Sea Research Part I: Oceanographic Research Papers, 48(11), 2347-2372.

Klein, P., & Coste, B. (1984). Effects of wind-stress variability on nutrient transport into the mixed layer. Deep Sea Research Part A. Oceanographic Research Papers, 31(1), 21-37.

Laanemets, J., Kononen, K., Pavelson, J., & Poutanen, E. L. (2004). Vertical location of seasonal nutriclines in the western Gulf of Finland. Journal of Marine Systems, 52(1-4), 1-13. https://doi.org/10.1016/j.jmarsys.2004.03.003

Lascaratos, A., Roether, W., Nittis, K., & Klein, B. (1999). Recent changes in deep water formation and spreading in the Eastern Mediterranean Sea: A review. Prog. Oceanogr., 44(1–3), 5–36. https://doi.org/10.1016/S0079-6611(99)00019-1

Lavigne, H., D'ortenzio, F., d'Alcalà, M. R., Claustre, H., Sauzède, R., & Gacic, M. (2015). On the vertical distribution of the chlorophyll a concentration in the Mediterranean Sea: a basin-scale and seasonal approach. Biogeosciences, 12(16), 5021-5039. https://doi.org/10.5194/bgd-12-4139-2015

Levy, M., Memery, L., & Madec, G. (1998). The onset of a bloom after deep winter convection in the northwestern Mediterranean sea: mesoscale process study with a primitive equation model. Journal of Marine Systems, 16(1), 7-21. https://doi.org/10.1016/S0924-7963(97)00097-3

Liu, C., Wang, P., Tian, J., & Cheng, X. (2008). Coccolith evidence for Quaternary nutricline variations in the southern South China Sea. Marine Micropaleontology, 69(1), 42-51. https://doi.org/10.1016/j.marmicro.2007.11.008

Longhurst, A. (1995). Seasonal cycles of pelagic production and consumption. Progress in oceanography, 36(2), 77-167.

Longhurst, A. R. (2006). Ecological Geography of the Sea, Second Edition, Academic Press, 2 Edn.

Lorbacher, K., Dommenget, D., Niiler, P. P., & Köhl, A. (2006). Ocean mixed layer depth: A subsurface proxy of ocean-atmosphere variability. Journal of Geophysical Research: Oceans, *111*(C7). https://doi.org/10.1029/2003JC002157

Lort J.M. (1977) Geophysics of the Mediterranean Sea Basins. In: Nairn A.E.M., Kanes W.H., Stehli F.G. (eds) The Ocean Basins and Margins (pp. 151-213). Springer, Boston, MA. https://DOI: 10.1007/978-1-4684-3036-3_4

Mancho, A. M., Hernández-García, E., Small, D., Wiggins, S., & Fernández, V. (2008). Lagrangian transport through an ocean front in the Northwestern Mediterranean Sea. Journal of Physical Oceanography, 38(6), 1222-1237. https://doi.org/10.1175/2007JPO3677.1

Marty, J. C., & Chiavérini, J. (2010). Hydrological changes in the Ligurian Sea (NW Mediterranean, DYFAMED site) during 1995–2007 and biogeochemical consequences. Biogeosciences, 7(7), 2117-2128. https://doi.org/10.5194/bg-7-2117-2010

Marty, J. C., Chiavérini, J., Pizay, M. D., & Avril, B. (2002). Seasonal and interannual dynamics of nutrients and phytoplankton pigments in the western Mediterranean Sea at the DYFAMED time-series station (1991–1999). Deep Sea Research Part II: Topical Studies in Oceanography, 49(11), 1965-1985.

Mayot, N., D'Ortenzio, F., Taillandier, V., Prieur, L., de Fommervault, O. P., Claustre, H., Bosse, A., Testor, P., & Conan, P. (2017). Physical and biogeochemical controls of the phytoplankton blooms in North Western Mediterranean Sea: A multiplatform approach over a complete annual cycle (2012–2013 DEWEX experiment). Journal of Geophysical Research: Oceans, 122(12), 9999-10019. https://doi.org/10.1002/2016JC012052

McGillicuddy, D. J., Jr., A. R. Robinson, D. A. Siegel, H. W. Jannasch, R. Johnson, T. D. Dickey, J. McNeil, A. F. Michaels, and A. H. Knap. (1998). Influence of mesoscale eddies on new production in the Sargasso Sea. Nature 394: 263-266.

Mignot, A., Claustre, H., Uitz, J., Poteau, A., D'Ortenzio, F., & Xing, X. (2014). Understanding the seasonal dynamics of phytoplankton biomass and the deep chlorophyll maximum in oligotrophic environments: A Bio-Argo float investigation. Global Biogeochemical Cycles, 28(8), 856-876.https://doi.org/10.1002/2013GB004781.

Millot, C. (1987). Circulation in the western Mediterranean-sea. Oceanologica Acta, 10(2), 143-149.

Millot, C. (1999). Circulation in the western Mediterranean Sea. Journal of Marine Systems, 20(1-4), 423-442. https://doi.org/10.1016/S0924-7963(98)00078-5

Morán, X. A. G., Taupier-Letage, I., Vázquez-Domínguez, E., Ruiz, S., Arin, L., Raimbault, P., & Estrada, M. (2001). Physical-biological coupling in the Algerian Basin (SW Mediterranean): influence of mesoscale instabilities on the biomass and production of phytoplankton and bacterioplankton. Deep Sea Research Part I: Oceanographic Research Papers, 48(2), 405-437. https://doi.org/10.1016/S0967-0637(00)00042-X

Obaton, D., Millot, C., Chabert d'Hières, G., and Taupier-Letage, I.: The Algerian Current: comparison between in situ and laboratory data set. Deep-Sea Res., 47, 2159–2190, 2000. https://doi.org/10.1016/S0967-0637(00)00014-5

Olita, A., Ribotti, A., Fazioli, L., Perilli, A., & Sorgente, R. (2013). Surface circulation and upwelling in the Sardinia Sea: A numerical study. Continental Shelf Research, 71, 95-108. https://doi.org/10.1016/j.csr.2013.10.011

Olita, A., Ribotti, A., Sorgente, R., Fazioli, L., & Perilli, A. (2011). SLA–chlorophyll-a variability and covariability in the Algero-Provençal Basin (1997–2007) through combined use of EOF and wavelet analysis of satellite data. Ocean Dynamics, 61(1), 89-102. https://doi.org/10.1007/s10236-010-0344-9

Pascual, M., Rives, B., Schunter, C., & Macpherson, E. (2017). Impact of life history traits on gene flow: A multispecies systematic review across oceanographic barriers in the Mediterranean Sea. PloS one, 12(5), e0176419.

Pasqueron de Fommervault, O., Migon, C., D'Ortenzio, F., Ribera d'Alcalà, M., & Coppola, L. (2015). Temporal variability of nutrient concentrations in the northwestern Mediterranean sea (DYFAMED time-series station). Deep-Sea Research Part I: Oceanographic Research Papers, 100, 1–12. https://doi.org/10.1016/j.dsr.2015.02.006

Pessini, F., Olita, A., Cotroneo, Y., & Perilli, A. (2018). Mesoscale eddies in the algerian basin: do they differ as a function of their formation site?. Ocean Science, 14(4), 669–688. https://doi.org/10.5194/os-14-669-2018

Pinot, J. M., Tintoré, J., & Gomis, D. (1995). Multivariate analysis of the surface circulation in the Balearic Sea. Progress in Oceanography, 36(4), 343–376. https://doi.org/10.1016/0079-6611(96)00003-1

Platt, T., Sathyendranath, S., Caverhill, C. M., & Lewis, M. R. (1988). Ocean primary production and available light: further algorithms for remote sensing. Deep Sea Research Part A, Oceanographic Research Papers, 35(6), 855–879. https://doi.org/10.1016/0198-0149(88)90064-7

Powley, H. R., Krom, M. D., & Van Cappellen, P. (2018). Phosphorus and nitrogen trajectories in the Mediterranean Sea (1950–2030): Diagnosing basin-wide anthropogenic nutrient enrichment. Progress in Oceanography, 162, 257-270. https://doi.org/10.1016/j.pocean.2018.03.003

Puillat, I., Taupier-Letage, I., & Millot, C. (2002). Algerian Eddies lifetime can near 3 years. Journal of Marine Systems, 31(4), 245–259. https://doi.org/10.1016/S0924-7963(01)00056-2

Ribera d'Alcalà, M., Civitarese, G., Conversano, F., & Lavezza, R. (2003). Nutrient ratios and fluxes hint at overlooked processes in the Mediterranean Sea. Journal of Geophysical Research: Oceans, 108(C9), 8106. https://doi.org/10.1029/2002JC001650

Rio, M. H., Pascual, A., Poulain, P. M., Menna, M., Barceló-Llull, B., & Tintoré, J. (2014). Computation of a new mean dynamic topography for the Mediterranean Sea from model outputs, altimeter measurements and oceanographic in situ data. Ocean Science, 10(4), 731–744. https://doi.org/10.5194/os-10-731-2014

Robinson, A. R., Leslie, W. G., Theocharis, A., & Lascaratos, A. (2001). Mediterranean sea circulation. Encyclopedia of Ocean Sciences, 1689-1705. https://doi.org/10.1016/B978-012374473-9.00376-3

Rohling, E. J., & Bryden, H. L. (1992). Man-induced salinity and temperature increases in Western Mediterranean Deep Water. Journal of Geophysical Research: Oceans, 97(C7), 11191-11198. https://doi.org/10.1029/92JC00767

Schroeder, K., Chiggiato, J., Bryden, H. L., Borghini, M., & Ben Ismail, S. (2016). Abrupt climate shift in the Western Mediterranean Sea. Scientific Reports, 6, 1–7. https://doi.org/10.1038/srep23009

Schroeder, K., Gasparini, G. P., Borghini, M., Cerrati, G., & Delfanti, R. (2010). Biogeochemical tracers and fluxes in the Western Mediterranean Sea, spring 2005. Journal of Marine Systems, 80(1-2), 8-24.

Schroeder, K., Ribotti, A., Borghini, M., Sorgente, R., Perilli, A., & Gasparini, G. P. (2008). An extensive western Mediterranean deep water renewal between 2004 and 2006. Geophysical Research Letters, 35(18). https://doi.org/10.1029/2008GL035146

Segura-Noguera, M., Cruzado, A., & Blasco, D. (2016). The biogeochemistry of nutrients, dissolved oxygen and chlorophyll a in the Catalan Sea (NW Mediterranean Sea). Scientia Marina, 80(S1), 39–56. https://doi.org/10.3989/scimar.04309.20A

Send, U., Font, J., Krahmann, G., Millot, C., Rhein, M., & Tintoré, J. (1999). Recent advances in observing the physical oceanography of the western Mediterranean Sea. Progress in Oceanography, 44(1-3), 37-64. https://doi.org/10.1016/S0079-6611(99)00020-8

Severin, T., Conan, P., Durrieu de Madron, X., Houpert, L., Oliver, M. J., Oriol, L., Caparros, J., Ghiglione, J., Pujo-Pay, M. (2014). Impact of open-ocean convection on nutrients, phytoplankton biomass and activity. Deep-Sea Research Part I: Oceanographic Research Papers, 94, 62–71. https://doi.org/10.1016/j.dsr.2014.07.015

Skliris, N., Zika, J. D., Herold, L., Josey, S. A., & Marsh, R. (2018). Mediterranean sea water budget long-term trend inferred from salinity observations. Climate Dynamics, 1-20. https://doi.org/10.1007/s00382-017-4053-7

Cronin, M. F., & Sprintall, J. (2009). Wind-and buoyancy-forced upper ocean. Encyclopedia of Ocean Sciences, 237-245.

Tanhua, T., Hainbucher, D., Schroeder, K., Cardin, V., Álvarez, M., & Civitarese, G. (2013). The Mediterranean Sea system: a review and an introduction to the special issue. Ocean Science, 9(5), 789-803. https://doi.org/10.5194/os-9-789-2013

Testor, P., & Gascard, J. C. (2005). Large scale flow separation and mesoscale eddy formation in the Algerian Basin. Progress in Oceanography, *66*(2-4), 211-230. https://doi.org/10.1016/j.pocean.2004.07.018

Urtizberea, A., Dupont, N., Rosland, R., & Aksnes, D. L. (2013). Sensitivity of euphotic zone properties to CDOM variations in marine ecosystem models. Ecological Modelling, 256, 16–22. https://doi.org/10.1016/j.ecolmodel.2013.02.010

Vargas-Yáñez, M., Zunino, P., Benali, A., Delpy, M., Pastre, F., Moya, F., Garcia-Martinez, M., Tel, E. (2010). How much is the western Mediterranean really warming and salting? Journal of Geophysical Research: Oceans, 115(4), 1–12. https://doi.org/10.1029/2009JC005816

Volpe, G., Nardelli, B. B., Cipollini, P., Santoleri, R., & Robinson, I. S. (2012). Seasonal to interannual phytoplankton response to physical processes in the Mediterranean Sea from satellite observations. *Remote Sensing of Environment*, *117*, 223-235. https://doi.org/10.1016/j.rse.2011.09.020

Waldman, R., Brüggemann, N., Bosse, A., Spall, M., Somot, S., & Sevault, F. (2018). Overturning the Mediterranean thermohaline circulation. Geophysical Research Letters, 45(16), 8407-8415. https://doi.org/10.1029/2018GL078502

Appendix 1

The appendix provides our routine for estimating the ND based on the nitracline and phosphacline in MATLAB.

```
%Calculate the vertical gradients
for p=1:7
for i=1:length(x_grid)
   for j=1:length(y_grid)-1
   str=['dNO3dz', num2str(p) ,'(j,i)=(z_' num2str(p), 'n(j,i)-z_', num2str(p),'n(j+1,i))/(y_grid(j)-
y_grid(j+1));'];
   eval(str)
   end
 end
end

for p=1:7
for i=1:length(x_grid)
   for j=1:length(y_grid)-1
   str=['dPO4dz', num2str(p) ,'(j,i)=(z_' num2str(p), 'p(j,i)-z_', num2str(p),'p(j+1,i))/(y_grid(j)-
y_grid(j+1));'];
   eval(str)
   end
end
end

%look for the maximum gradient
 p=5
for i=1:length(x_grid)
   str=['j=find(dNO3dz', num2str(p),'(:,i)==max(dNO3dz',num2str(p),'(:,i)));'];
   eval(str)
   str=['depth_n',num2str(p),'(i)=y_grid(j);'];
   eval(str)
   str=['conc_n', num2str(p),'(i)=z_', num2str(p),'n(j,i); '];%calculate the concentration of the
nutrient at the nutricline)
   eval(str)
end

for i=1:length(x_grid)
   str=['j=find(dPO4dz', num2str(p),'(:,i)==max(dPO4dz',num2str(p),'(:,i)));'];
   eval(str)
   str=['depth_p',num2str(p),'(i)=y_grid(j);'];
   eval(str)

   str=['conc_p', num2str(p),'(i)=z_', num2str(p),'p(j,i); '];%calculate the concentration of the
nutrient at the nutricline)
   eval(str)
end

%plots
figure
subplot(121)
```

```
pcolor(x_grid,-y_grid(1:end-1),dPO4dz1)
shading flat
hold on
plot(x_grid, -depth_p1,'k')

subplot(122)
pcolor(x_grid,-y_grid(1:end-1),dNO3dz1)
shading flat
hold on
plot(x_grid, -depth_n1,'k')

%and so on for the other cruises
```

Appendix 2

The appendix provides our routine for plotting DCM, MLD and NC for each cruise in MATLAB.

```
figure (1)

%first cruise
clc
plot(x_grid,-depth_n1)
hold on
plot(x_grid,-depth_p1,'r')
plot(dcm1(:,1),dcm1(:,2),'.-k')
plot(meanMLD1(:,2),meanMLD1(:,3),'.-g')
titolo = 'spring 2005'
xlabel('Longitude')
ylabel('depth (m)')
title(titolo);
legend('nitracline','phosphacline','dcm','mld');
ylim([-225 0])
grid on

figure (2)
%second cruise
plot(x_grid,-depth_n2)
hold on
plot(x_grid,-depth_p2,'r')
%dcm2=0
plot(dcm2(:,1),dcm2(:,2),'.-k')
plot(meanMLD2(:,2),meanMLD2(:,3),'.-g')
titolo = 'summer 2006'
xlabel('Longitude')
ylabel('depth (m)')
title(titolo);
legend('nitracline','phosphacline','dcm','mld');
 ylim([-225 0])
grid on

 figure (3)
%Third cruise
```

```
plot(x_grid,-depth_n3)
hold on
plot(x_grid,-depth_p3,'r')
plot(dcm3(:,1),dcm3(:,2),'.-k')
plot(meanMLD3(:,2),meanMLD3(:,3),'.-g')
titolo = 'autumn 2007'
xlabel('Longitude')
ylabel('depth (m)')
title(titolo);
xlabel('Longitude')
ylabel('depth (m)')
 legend('nirtacline','phosphacline','dcm','mld');
 ylim([-225 0])
grid on

figure (4)
 %Fourth cruise
plot(x_grid,-depth_n4)
hold on
plot(x_grid,-depth_p4,'r')
plot(dcm4(:,1),dcm4(:,2),'.-k')
plot(meanMLD4(:,2),meanMLD4(:,3),'.-g')
titolo = 'spring 2010'
title(titolo);
xlabel('Longitude')
ylabel('depth (m)')
legend('nirtacline','phosphacline','dcm','mld');
 ylim([-225 0])
grid on

 figure (5)
%Fifth cruise
plot(x_grid,-depth_n5)
hold on
plot(x_grid,-depth_p5,'r')
plot(dcm5(:,1),dcm5(:,2),'.-k')
plot(meanMLD5(:,2),meanMLD5(:,3),'.-g')
titolo = 'autumn 2011';
title(titolo);
xlabel('Longitude')
ylabel('depth (m)')
 legend('nirtacline','phosphacline','dcm','mld');
 ylim([-225 0])
 grid on

 figure (6)
%Sixth cruise
plot(x_grid,-depth_n6)
hold on
plot(x_grid,-depth_p6,'r')
plot(dcm6(:,1),dcm6(:,2),'.-k')
plot(meanMLD6(:,2),meanMLD6(:,3),'.-g')
```

```
titolo = 'winter 2012';
title(titolo);
xlabel('Longitude')
ylabel('depth (m)')
legend('nirtacline','phosphacline','dcm','mld');
ylim([-225 0])
 grid on


 figure (7)
%Seventh cruise
plot(x_grid,-depth_n7)
hold on
plot(x_grid,-depth_p7,'r')
plot(dcm7(:,1),dcm7(:,2),'.-k')
plot(meanMLD7(:,2),meanMLD7(:,3),'.-g')
titolo = 'summer 2015';
title(titolo);
xlabel('Longitude')
ylabel('depth (m)')
legend('nirtacline','phosphacline','dcm','mld');
ylim([-225 0])
grid on
```

Appendix 3

The appendix provides our routine for reading the ODV downloaded interpolated dataset (x, y, z variables) in MATLAB.

The routine reads a text file produced by ODV in the ODV spreadsheet format, and produces an output cell var. This program keeps only the values that contain latitude, longitude, depth, potential temperature, salinity, potential density. Modified by Antonio Petrizzo, ISMAR VE, 2018 from Vassilis Zervakis and Stallo Leontiou, Mytilene, University of the Aegean, 2010.

```
%Function myhydro = ODVTXTread(infile)
% Usage output = ODVTXTread(infile)
%fid = fopen(infile);
%strline = fgetl(fid);
%hydrodata = [];
%contStaz = 0;
while strline ~= -1
   if strline(1:2) == '//'
      strline = fgetl(fid);
      %disp('//')
   else
      if strline(1:6) == 'Cruise'
         strline = fgetl(fid);

      end
      if strline(1) == '  '
         %disp('values')
         % find where in the line there are tabs
         jtabs = [];
```

```
   jtabs = find(strline ~= '   ');
   % find the parts where non-tabs are continuous (so they contain
   % data)
   ilast = max(jtabs);
   istart = min(jtabs);
   ivalues = 0;
   i = 1;
   ibegin = i;
   numtimes = 0;
   while(jtabs(i) < ilast)
      ivalues = ivalues + 1;
      if jtabs(i)+1 == jtabs(i+1)
         i = i+1;
      else
         numtimes = numtimes+1;
         iend = i;
         value = strline(jtabs(ibegin):jtabs(iend));
         i = i + 1;
         ibegin = i;
         if numtimes == 1
            depth = str2num(value);
         end
         if numtimes == 3
            sal = str2num(value);
         end
         if numtimes == 5
            temp = str2num(value);
         end
         if numtimes == 7
            pdens = str2num(value);

         if ((isfinite(temp)) & (temp ~= 1.))
            dat = [lat long depth temp sal pdens];
            if (length(lat) > 1)
               lat;
            end
            hydrodata = [hydrodata ; dat];
            myhydro{contStaz} = hydrodata;
         end
         numtimes = 0;
         end
      end
   end
else
   % find where in the line there are tabs
   jtabs = [];
   jtabs = find(strline ~= '   ');
   % find the parts where non-tabs are continuous (so they contain
   % data)
   ilast = max(jtabs);
   istart = min(jtabs);
   ivalues = 0;
```

```
        i = 1;
        ibegin = i;
        numtimes = 0;
        jtabs;
        while(jtabs(i) < ilast),
          ivalues = ivalues + 1;
          if jtabs(i)+1 == jtabs(i+1),
            i = i+1;
          else
            numtimes = numtimes+1;
            iend = i;
            value = strline(jtabs(ibegin):jtabs(iend));
            i = i + 1;
            ibegin = i;
            if numtimes == 5,
              long = str2num(value);
            end
            if numtimes == 6,
              lat = str2num(value);
              A = [lat long];
              contStaz = contStaz + 1;
              hydrodata = [];
            end
          end
        end
      end
    end
    strline = fgetl(fid);
end
fclose(fid);
 return
```

Appendix 4

The appendix provides our routine for estimating the MLD in MATLAB, by the application of the Lorbacher et al. (2006) MLD method, using the data set provide by the CNR and ISMAR Cruises from 2005 - 2015 (seven cruises).

```
%parameter
depth = 3;
ptemp = 4;
sal = 5;
pdens = 6;

%select which to use
par = sal;
titolo = '(#cruise_file)cruise';
inputFile = pc_dir_'(cruise_file) '.txt';
outputDir = file on the pc where is wanted to keep the information generated;
switch par
```

```
   case sal
      times = 10.;
      nomeGraf = 'sal';
      asseX = 'salinity (PSU)';
      leg = 'Salinity';
   case pdens
      times = 4.;
      nomeGraf = 'pdens';
      asseX = 'potential density (kg/m^3)';
      leg = 'Potential Density';

   otherwise
      times = 1;
      nomeGraf = 'ptemp';
      asseX = 'potential temperature';
      leg = 'Potential Temperature (degrees Celsius)';

end

%read data plot my graphs
mydata = ODVTXTread(inputFile);
nstaz = length(mydata);
for i =1:nstaz
   z = -mydata{1,i}(:,3);
   t = mydata{1,i}(:,par)*times;
   [mld(i), qe(i), imf(i), gt{i}, sig30{i}, res{i}] = lorbacher_mixed_depth(z,t);
   f = figure;
   plot(t/times,z,'k','Linewidth',1)%
  %---------------------
  hold on
   mld_depth=mld(:,i);
    m1=min((t/times)-1.5);
    m2=max(t/times);


  plot([m1 m2],[mld_depth mld_depth],'r-','Linewidth',2)
   leg2 = 'Mix Layer Depth'
    %-------------------------
   ylim([-100 0])
   legend(leg,leg2,'location','southwest')
   xlabel(asseX)
   ylabel('depth (m)')
   title(titolo);

   %baseFileName = sprintf('figure_%d.jpg',i);
   % Specify some particular, spDecific folder:
   graf = [outputDir titolo '_' nomeGraf '_staz_' num2str(i)];
   saveas(f,graf,'tiff')
   close(f)
end

fpath=…\MLD_scripts\MLD_allcruises';
```

```
f = figure;
plot(mld,'r-*')
saveas(f,[outputDir 'mld'],'tiff')
close(f)

save([outputDir titolo '_' nomeGraf '_mld_' ],'mld')
```